

NASA CR-54150

STUDY PROGRAM TO IMPROVE FUEL CELL PERFORMANCE BY PULSING TECHNIQUES

by

M. L. KRONENBERG
K. V. KORDESCH

Prepared for

NATIONAL AERONAUTICS AND SPACE ADMINISTRATION
CONTRACT NAS3-2752

OTS PRICE

XEROX

MICROFILM

\$

\$

4600 ph.

FACILITY FORM 802

N64-28086

(ACCESSION NUMBER)

(PAGES)

Cr-54150

(NASA CR OR TMX OR AD NUMBER)

(THRU)

(CODE)

(CATEGORY)

UNION CARBIDE CORPORATION

FINAL REPORT

STUDY PROGRAM TO IMPROVE FUEL CELL
PERFORMANCE BY PULSING TECHNIQUES

by

M. L. Kronenberg
K. V. Kordes

prepared for

NATIONAL AERONAUTICS AND SPACE ADMINISTRATION

June 28, 1964

CONTRACT NAS3-2752

Technical Management
NASA Lewis Research Center
Cleveland, Ohio
W. J. Nagle

UNION CARBIDE CORPORATION
DEVELOPMENT DEPARTMENT
PARMA RESEARCH LABORATORY
PARMA, OHIO

TABLE OF CONTENTS

	<u>Page</u>
LIST OF ILLUSTRATIONS	ii
ABSTRACT	1
1. 0 SUMMARY	1
2. 0 INTRODUCTION	2
3. 0 MEETINGS OR CONFERENCES	4
4. 0 FACTUAL DATA	5
APPENDIX (Figures 1 through 29)	15

LIST OF ILLUSTRATIONS
(APPENDIX)

<u>Figure</u>	<u>Title</u>
1	Drawing of Teflon Cell Used for Electrolyte and Gas Pulsing.
2	Drawing of Stainless Steel Electrode Holder and Gas Chamber.
3	System for Subsonic Gas and Electrolyte Pulsing.
4	Electrode-Reference Potential as a Function of Pulsing Speed; for 1/4-Inch Carbon Electrodes.
5	Electrode-Reference Potential as a Function of Pulsing Speed; for Thin, Composite Electrodes.
6	Electrode-Reference Potential as a Function of Pulsing Speed; Metal Anode and Cathode (Amplitude Range: 10 - 22).
7	Electrode-Reference Potential as a Function of Pulsing Speed; Metal Anode and Cathode (Amplitude Range: 13 - 18).
8	Anode-Reference Polarization Curves; Before, During and After Pulsing 1/4-Inch Carbon Electrodes.
9	Cathode-Reference Polarization Curves; Before, During and After Pulsing 1/4-Inch Carbon Electrodes.
10	Anode-Cathode Polarization Curves; Before, During and After Pulsing.
11	Oscilloscope Trace of Anode-Reference Potential Fluctuations During Mechanical Pulsing of Electrolyte.
12	Oscilloscope Trace of Cathode-Reference Potential Fluctuations During Mechanical Pulsing of Electrolyte.
13	Polarization Curves Before, During and After Vibration Tests; IR-Free.
14	Polarization Curves Before, During and After Vibration Tests; IR-Included.
15	IR-Free Voltage vs. Vibration Amplitudes at Constant Current and Constant Frequency of 60 Cyc/Sec.
16	IR-Included Voltage vs. Vibration Amplitudes at Constant Current and Constant Frequency of 60 Cyc/Sec.
17	Cell Voltage vs. Vibration Frequency for Three Types of Electrodes.
18	Equipment for Sonic Pulsing of Electrolyte.
19	Effect of Electrolyte Pulsations on Cell Voltage for Metal, 1/4-Inch Carbon, and Thin-Composite Electrodes.
20	Variable Rate Timer Switch.

LIST OF ILLUSTRATIONS
(Continued)

<u>Figure</u>	<u>Title</u>
21	Circuit Used for Interrupted D. C.
22	Interrupted D. C. Wave For. (300 cps, Avg. Current 100 ma).
23	Circuit Diagram for A. C. Superimposed on D. C.
24	Wave Form of A. C. Superimposed on D. C. - 50 ma D. C. , 10 ma Superimposed A. C.
25	Dual-Range Constant Current Interrupter (Timer Controlled).
26	Cell Voltage vs. Frequency of Interrupted d. c. for Metal Electrodes.
27	Effect of Heavy Discharge Pulse on Cell Voltage
28	Comparison Heavy Discharge Pulse and Normal Discharge
29	Cell Voltage Maintained by Heavy Discharge Pulse.

STUDY PROGRAM TO IMPROVE FUEL CELL PERFORMANCE BY PULSING TECHNIQUES

by M. L. Kronenberg and K. V. Kordesch

ABSTRACT

This investigation was concerned with the effect of the modification of the gas-electrolyte interface on the performance of fuel cell electrodes. Modification of the interface was accomplished by subjecting the porous electrodes to electrical and mechanical pulses at subsonic and sonic frequencies. Hydrophobic and hydrophilic electrodes were used in this investigation.

* * * * *

1.0 SUMMARY

This investigation was concerned with the effect of the modification of the gas-electrolyte interface on the performance of fuel cell electrodes. Modification of the interface was accomplished by subjecting the porous electrodes to electrical and mechanical pulses at subsonic and sonic frequencies. Three types of fuel cells were studied: carbon, metal, and a thin-composite electrode employing an electrochemically active carbon zone on a porous metal backing material.

Low frequency (0-450 cpm), high amplitude (9 - 24 psia) electrolyte pulses occasionally produced small changes in the performance of all three types of electrodes. These changes were attributed to an accelerated development of the three-phase reaction zone (positive effect) or accelerated wetting (negative effect). Metal anodes normally showed increased polarization at high pulsing amplitudes. Pulsing of the electrolyte at sonic frequencies had a negligible effect on performance.

Fuel cell performance on all three types of electrodes was not affected by electrode vibration tests conducted at frequencies ranging from 20 to 300 cps.

Four different modes of electrical pulsing were investigated: interrupted d. c. ; a. c. superimposed on d. c. ; charge-discharge cycling; and heavy discharge pulsing. The first three had no significant effect on electrode life or performance but very significant effects were observed with heavy discharge pulsing. In certain instances polarization was reduced by as much as 100 mv by the periodic application of short discharge pulses (e. g. 2-second pulses of a current density of 500 ma/cm² every few minutes). These improvements may be related to catalyst reactivation. This heavy-discharge type pulsing will be investigated in more detail in the future, especially since it became apparent that even pulses applied only once a day showed improvements.

2.0 INTRODUCTION

Power density available from a fuel cell is limited by a large number of factors. The purpose of this investigation was to consider which, if any, of these limiting factors is sensitive to pulsed operation and to determine whether some mode of pulsed operation could be used to increase power output or extend the useful life of fuel cells.

One possible limitation is high activation polarization, resulting from catalyst ineffectiveness. Such a condition may result from a basically poor catalyst choice, deterioration of catalyst activity with usage, or an inadequate electrochemical surface area. Under certain conditions catalyst activity could be restored and active surface area increased by electrical and/or mechanical pulsing. If, for example, the active catalyst is an oxide operating in a reducing atmosphere, the periodic reoxidation of the catalyst by chemical or electrical means could serve to reactivate the catalyst. Also, mechanical pulsing of the gas or electrolyte phase could periodically expose fresh catalyst surface or additional three-phase reaction sites. Increasing the electrochemically useful area in this way would aid even poorly catalyzed electrodes.

A second basic limitation to power density is concentration polarization. This phenomenon results from the depletion (or accumulation) of ions at a rate in excess of the diffusion rate of ions into the electrolyte. It is

well known that such polarization can be reduced by mechanical stirring, as is practiced in electroplating, for example. Such agitation could, in principle, be introduced by periodic disturbance of the fuel cell electrolyte/electrode interface by means of large amplitude and low frequency pulses. On the other hand, too high frequency pulses introducing only oscillations in the electrolyte of an amplitude small when compared to the dimensions of the electrode micropores, would have no appreciable effect on concentration polarization. In this context, even 60-cycle/sec. pulsing would have to be considered a fairly "high" frequency.

A closely related phenomenon occurs when a reactant gas is being consumed more rapidly than it can diffuse through the electrode to the zone of electrochemical reaction. For pure gas reactants, such as hydrogen and oxygen, this current density limit set by gaseous diffusion occurs at current density values far in excess of normal operating levels (equivalent to thousands of amperes per square foot). In operation with impure reactants, such as air, a high concentration polarization due to reactant (oxygen) depletion can occur--the result of build-up of an inert blocking layer of nitrogen. In this case, pulsing of the fuel cell should have beneficial results.

One inescapable limitation on power density is the internal ohmic resistance; this should be insensitive to pulsed operation, except for the usually small portion of the total resistance due to contacts. (Vibration can sometimes lower the resistance of a poor contact or remove gas bubbles from the interface.)

Summarizing the foregoing discussion, there were reasons to believe that pulsed operation of a fuel cell could produce major changes in useful current or voltage for electrode systems showing high activation or concentration polarization.

Pulsing effects were studied on three types of fuel cell electrodes: carbon, metal, and a thin, composite electrode employing an electrochemically active carbon zone on a porous metal substrate. This permitted the results to be obtained on three quite dissimilar electrode surfaces and broadened the generality of any conclusions arrived at in the study. The experimental design involving three electrode types and three modes of

pulsing (mechanical, sonic and electrical). The observed variable was normally the polarization curve. Controlled variables included, among others, the intensity and frequency of pulsing. However, in certain instances it was more appropriate to maintain the cell at constant current and observe the effect on the cell voltage, and of changing the frequency or intensity of the pulse.

Pulsed cells and unpulsed control cells were placed on long-term life tests for the instrumentally simple case of electrical pulsing to look for possible long-term or accumulative effects.

3.0 MEETINGS AND CONFERENCES

1) G. E. Evans, K. V. Kordesch, and M. L. Kronenberg met with W. J. Nagle, Project Supervisor from NASA on 24 June, 1963 to discuss the scope and program of the contract. It was agreed that initial studies would involve the application of mechanical and electrical pulses that could change the position of the gas-electrolyte interface within the electrodes.

2) G. E. Evans, K. V. Kordesch, and M. L. Kronenberg of Union Carbide met with E. M. Cohen, R. L. Cummings, H. S. Schwartz and W. J. Nagle of NASA at Union Carbide Parma Research Laboratory on 16 December, 1963 to discuss the progress and scope of the contract. The meeting was continued on the following day with Prof. T. J. Gray of Alfred University and several other members of the NASA staff also present. The purpose of this second meeting was to provide an opportunity for a free exchange of ideas between Prof. Gray (who is investigating pulsing at porous electrodes) and members of Union Carbide and NASA who are interested in pulsing studies on porous electrodes.

3) On 13 February, 1964, K. V. Kordesch and M. L. Kronenberg of Union Carbide visited the laboratories of Prof. T. J. Gray at Alfred University. The purpose of the visit was to observe Gray's preparation of metal electrodes and to help determine whether this type of electrode would be a suitable hydrophilic electrode for pulse testing.

4.0 FACTUAL DATA

4.1 Mechanical Motion of Electrolyte

4.1.1 Test Equipment

A drawing of the cell which was designed and built for subsonic electrolyte pulsing is shown in Figure 1. The cell was initially made of Teflon but later remade of clear polystyrene to permit observation of electrodes during assembly. Accesses to the electrolyte room are for filling, pressure readings, and reference electrode. A drawing of the stainless steel holders and gas room is shown in Figure 2. An O-ring gasket between the electrode and cell housing prevents the electrolyte from penetrating around the electrode.

For electrolyte pulsing in the subsonic range, a 1/8-h. p. motor with a gear box for varying speeds was coupled with a piston over an eccentric cam arrangement to provide controlled amplitudes and frequencies. Electrolyte pulsations from 0 to 450 cycles/minute at amplitudes high enough to displace liquids throughout the total electrode thickness was provided by the system shown in Figure 3. The pressure on the electrolyte was varied from 9 to 24 psi. The pressure fluctuations were measured with a Marsh pressure gage (stainless steel Bourdon tube).

4.1.2 Experimental Results

The normal procedure was to run a polarization curve before pulsing, followed by the pulsing experiment performed under constant current conditions, and a polarization curve after pulsing. Figures 4 and 5 show the effect of pulsing on 1/4-inch and 0.045-inch anodes and cathodes at a constant current of 40 ma/cm² for pulsing frequencies scanning the range of 0 to 340 cpm. Figures 6 and 7 show similar curves for a metal anode and cathode* at a constant current of 15 ma/cm² over the same pulsing frequencies. The voltage readings are resistance-free values taken with a 60-cycle interrupter. Unless specified, the anode fuel is hydrogen and the cathodic fuel is oxygen. The

* The 1/4-inch all-carbon, and thin composite (carbon-metal) electrodes were supplied by Union Carbide Corporation, Development Department, for test purposes. The metal electrodes reported herein were prepared from dual-porosity Ni sheet from SKC Associates made with 49% voids, 0.259 inch in thickness and catalyzed as follows: (1) soak in 2% PtCl₄-2% PdCl₂ for half-an-hour; (2) plate for 6 minutes at 25 ma/cm²; (3) reduce in 10% hydrazine soln.; (4) wash copiously and dry. (This is a slight modification of the procedure recommended by Prof. Gray.)

data presented in Figs 4 and 5 for all-carbon electrodes and composite electrodes were reproducible, while results on metal electrodes were not consistent. The two readings given at 0 cpm represent measurements before and after pulsing. 12-Normal KOH was used in all experiments.

Figures 8 through 10 show resistance-included polarization curves taken before, during, and after pulsing on 1/4-inch carbon electrodes at two pressure amplitude settings. Figures 11 and 12 show oscilloscope traces of anode-reference potential fluctuations and cathode-reference potential changes during pulsing. The vertical scale is 5 mv/cm, sweep time 2 sec./cm, and the pump speed 55 cpm. The voltage variations observed during a pump cycle amounted to less than 2 mv. Drifting was observed in the anodic potential in this and several other instances, but not in the cathodic potential.

All data pertinent to mechanical pulsing of the electrolyte are tabulated in Table I. The results were obtained at a current density of 40 ma/cm² for carbon and composite electrodes, and 10 and 15 ma/cm² for metal electrodes. The far-right columns show the changes in electrode potential that resulted from the pulsing, i. e., the mv difference between initial potential and potential during and after pulsing. A positive difference denotes improved performance for both anodes and cathodes.

On the basis of the data obtained (Figs. 4 through 12, Table I), the following conclusions were reached:

(1) Only relatively small effects were observed (normally several mv or less) from electrolyte pulsing on carbon and composite electrodes under the conditions described.

(2) Polarization of anodes normally increases during pulsing. This appears to be especially true for metal anodes at high pulsing amplitudes.

(3) Only relatively minor beneficial effects were occasionally noted from pulsing. An explanation for this effect is the acceleration of the development of a 3-phase zone. Electrodes do not normally reach optimum performance immediately upon starting up but require a "breaking-in" period which may be accelerated by pulsing.

TABLE I

MECHANICAL PULSING DATA FOR ELECTROLYTE

Electrode	Pulsing Speed (cpm)	Pressure Range (psia)	Potential (volts)			Potential Change(mv)	
			Initial	During	After	During	After
1/4" Anode-Carbon (40 ma/cm ²)	56	13-23	0.475	0.477	0.484	-2	-9
	112	13-22	0.475	0.482	0.484	-7	-9
	170	11-21	0.475	0.483	0.484	-8	-9
	243	10-23	0.475	0.484	0.484	-9	-9
	341	9-24	0.475	0.484	0.484	-9	-9
1/4" Cathode-Carbon (40 ma/cm ²)	56	13-23	1.324	1.320	1.340	-4	+16
	112	13-22	1.324	1.323	1.340	-1	+16
	170	11-21	1.324	1.325	1.340	+1	+16
	243	10-23	1.324	1.325	1.340	+1	+16
	341	9-24	1.324	1.326	1.340	+2	+16
1/4" Cathode-Carbon (Air, 40 ma/cm ²)	56	12-19	1.273	1.277	1.277	+4	+4
	112	11-22	1.273	1.277	1.277	+4	+4
	170	11-23	1.273	1.278	1.277	+5	+4
	243	10-23	1.273	1.279	1.277	+6	+4
	341	10-23	1.273	1.279	1.277	+6	+4
Anode-Composite (40 ma/cm ²)	56	13-22	0.513	0.517	0.527	-4	-14
	112	12-22	0.513	0.519	0.527	-6	-14
	170	12-22	0.513	0.521	0.527	-8	-14
	243	11-23	0.513	0.522	0.527	-9	-14
	341	11-23	0.513	0.522	0.527	-9	-14
Cathode-Composite (40 ma/cm ²)	56	13-22	1.327	1.324	1.330	-3	+3
	112	12-22	1.327	1.327	1.330	0	+3
	170	12-22	1.327	1.329	1.330	+2	+3
	243	11-23	1.327	1.330	1.330	+3	+3
	341	11-23	1.327	1.331	1.330	+4	+3
Cathode-Composite (Air, 40 ma/cm ²)	56	13-22	1.285	1.284	1.275	-1	-10
	112	12-22	1.285	1.284	1.275	-1	-10
	170	12-22	1.285	1.283	1.275	-2	-10
	243	11-23	1.285	1.282	1.275	-3	-10
	341	11-23	1.285	1.282	1.275	-3	-10
Anode - Metal (10 ma/cm ²)	56	11-18	0.469	0.470	0.471	-1	-2
	112	11-18	0.469	0.471	0.471	-2	-2
	170	10-18	0.469	0.471	0.471	-2	-2
	243	10-18	0.469	0.476	0.471	-7	-2
	341	9-22	0.469	0.479	0.471	-10	-2
	450	9-22	0.469	0.478	0.471	-9	-2
Cathode - Metal (10 ma/cm ²)	56	11-18	1.384	1.384	1.386	0	+2
	112	11-18	1.384	1.385	1.386	+1	+2
	170	10-18	1.384	1.386	1.386	+2	+2
	243	10-18	1.384	1.386	1.386	+2	+2
	341	9-22	1.384	1.387	1.386	+3	+2
	450	9-22	1.384	1.387	1.386	+3	+2

(Continued)

TABLE I
(Continued)

Electrode	Pulsing Speed (cpm)	Pressure Range (psia)	Potential (volts)			Potential Change(mv)	
			Initial	During	After	During	After
Anode - Metal (15 ma/cm ²)	56	12-18	0.501	0.496	0.494	+5	+7
	112	12-19	0.501	0.506	0.494	-5	+7
	170	11-19	0.501	0.513	0.494	-13	+7
	243	11-20	0.501	0.525	0.494	-24	+7
	341	10-21	0.501	0.555	0.494	-54	+7
Cathode - Metal (15 ma/cm ²)	56	12-18	1.358	1.342	1.343	-16	-15
	112	12-19	1.358	1.348	1.343	-10	-15
	170	11-19	1.358	1.349	1.343	-9	-15
	243	11-20	1.358	1.353	1.343	-5	-15
	341	10-21	1.358	1.357	1.343	-1	-15
Anode - Metal (15 ma/cm ²)	56	14-17	0.511	0.496	0.511	+16	0
	112	14-17	0.511	0.496	0.511	+16	0
	170	14-18	0.511	0.496	0.511	+16	0
	243	14-18	0.511	0.504	0.511	+7	0
	341	13-18	0.511	0.510	0.511	+1	0
Cathode - Metal (15 ma/cm ²)	56	14-17	1.351	1.362	1.353	+11	+2
	112	14-17	1.351	1.356	1.353	+5	+2
	170	14-18	1.351	1.358	1.353	+7	+2
	243	14-18	1.351	1.358	1.353	+7	+2
	341	13-18	1.351	1.358	1.353	+7	+2

4.2 Mechanical Motion of Electrodes.

4.2.1 Test Equipment.

Vibration tests were conducted on all three types of electrodes in three different ways: 1) by coupling the plunger of a continuous-duty solenoid directly to the electrode backing plate and driving the system at 60 cycles, controlling the input power by means of a Variac; 2) by mounting on a light vibration table and vibrating the complete cell at several different amplitudes in the range of 20 to 200 cps by means of a signal generator and power amplifier; 3) by mounting the cell on a support coupled to a compressed-air vibrator* which operates over the range 160-300 cps.

4.2.2 Experimental Results.

In the course of determining vibration effects, polarization curves were taken before, during and after vibration, as in Figs. 13 and 14. Variations of the vibration amplitude (adjusted by Variac setting) at constant current

* CV-19 Vibrator, Martin Engineering Co., Neponset, Illinois.

and constant frequency are shown in Figs. 15(IR-free) and 16(IR-included). Changes in the vibration frequency at constant amplitude and constant current are presented in Fig. 17.

It is apparent from Figs. 13 - 17 that the electrodes are virtually insensitive to vibrations because in no instance did the resistance-free or resistance-included cell voltages change by more than several millivolts for the 1/4-inch, the thin-composite, or the metal electrodes over these frequency ranges.

4.3 Sonic Pulsing.

4.3.1 Test Equipment

Equipment for pulsing the electrolyte at sonic frequencies is shown in Fig. 18. A diaphragm at the bottom of the Teflon cell (1) is vibrated by means of an audio-driver unit (2). A signal generator (3) and amplifier (4) provide frequency-controlled power to the driver unit. The pressure fluctuations are sensed by a Bourdon tube-transducer combination (5) which is controlled by another signal generator (6). Pressure fluctuations are read on the oscilloscope (7) as voltage readings. The transducer was not fast enough to follow pressure fluctuations at high frequencies, therefore, experimental verification of electrolyte pulsing at sonic frequencies was obtained by means of a crystal pickup.

4.3.2 Experimental Results.

Tests were run at frequencies ranging from 20 to 20,000 cps at two amplitude settings (40 and 80, 20 DB) on all three types of electrodes. The tests were run (as shown in Fig. 19) at several constant current densities and the frequency was scanned over the sonic range. No change in cell voltage resulted from pulsing over the entire range. The sensitivity of the voltage measurement was 0.001 volt.

4.4 Electrical Pulsing.

4.4.1 Test Equipment.

Fuel cell electrodes were run under four different conditions: interrupted d. c. ; a. c. superimposed on d. c. ; charge-discharge cycling; and heavy discharge pulsing.

4.4.1.1 Interrupted D. C.

The low frequency-interrupted d. c. was obtained using the variable rate timer switch shown in Fig. 20. This device permitted on-off switching from 1 second to 10 minutes. Sixty-cycle pulsing was accomplished by means of a Kordesch-Marko interrupter^{*}. The circuit used to obtain interrupted d. c. at sonic frequencies is shown in Fig. 21. The magnitude and wave form of the resulting current, as shown in Fig. 22, was obtained by feeding the voltage across a 1-ohm precision resistor into a Tektronix 535A Oscilloscope.

4.4.1.2 A. C. Superimposed on D. C.

The circuit used to produce a. c. superimposed in the range of 20 to 20,000 cycles per second is shown in Fig. 23. A Hewlett-Packard 201-B sine wave signal generator was used and the current wave form and frequencies were observed with a Tektronix 535-A Oscilloscope. The wave form for 50 ma d. c. with superimposed a. c. of 10 ma at 1000 cps is shown in Fig. 24 as an example of the wave form observed.

4.4.1.3 Charge-Discharge Cycling.

Charge-discharge cycling was accomplished by using the variable rate timer described in Section 4.4.1.1 above.

4.4.1.4 Heavy-Discharge Pulsing.

The block diagram of a specially designed pulsing instrument is shown in Fig. 25. This instrument will provide controlled heavy-discharge pulses up to 4 amps from 0.2 to 5 seconds duration and low current pulses up to 0.5 amps of 1 second to 15 minutes duration. The system also permits an open circuit of 1 or 2 seconds duration to follow the heavy pulse. The instrument can be used for resistance-free or resistance-included measurements.

4.4.2 Experimental Results.

Results of interrupted d. c. and charge-discharge cycling experiments for the three types of electrodes are summarized in Table II. A control cell run with continuous d. c. was run at the same time as each test cell on pulsed d. c. Only one result is given for long-term testing of metal electrodes because

^{*} A description of the 60-cycle Kordesch-Marko interrupter can be found in J. Electrochem. Soc., Vol. 107, pp480-483, June 1960.

TABLE II
RESULTS OBTAINED FROM ELECTRICAL PULSING EXPERIMENTS

Type of Electrode	Cycle	No. Days on Test	Average Current Density (ma/cm ²)	Initial Potential		Final Potential		mv Change from	
				Control	Test	Control	Test	Control	Test
1/4-Inch Carbon	60 cycle/sec. Interrupted	20	10	.898	.902	.939	.936	+41	+34
"	"	20	50	.846	.843	.863	.858	+17	+15
"	"	15	10	.947	.953	.939	.921	-8	-32
"	"	15	50	.899	.897	.862	.863	-37	-34
"	"	26	10	.953	.913	.960	.912	+7	-1
"	"	26	50	.915	.879	.884	.861	-31	-18
"	6 sec. on - 6 sec. off	15	50	.890	.887	.814	.839	-76	-48
"	"	15	50	.887	.887	.854	.839	-33	-48
"	5 minute discharge 10 sec. charge	28	25 discharge, 2.5 charge	.854	.839	.743	.749	-111	-90
"	300 cycle/sec. Interrupted	13	50	.825	.824	.880	.866	+55	+42
Thin Electrodes, Normal Wetproofing	60 cycle/sec. Interrupted	22	10	.939	.933	.949	.946	+10	+13
"	"	22	50	.892	.900	.909	.885	+17	-15
Thin Electrodes, Heavy Wetproofing	"	22	10	.904	.897	.910	.877	+6	-10
"	"	22	50	.799	.806	.788	.771	-9	-35
Thin Electrodes, Normal Wetproofing	5 minute discharge, 10 sec. charge	20	25 discharge, 2.5 charge	.851	.833	.880	.790	+29	-43
"	"	20	"	.851	.849	.880	.811	+29	-38
"	"	15	"	.819	.780	.833	.846	+14	+66
"	"	15	"	.785	.799	.859	.834	+74	+35
Thin Electrodes, Normal Wetproofing	300 cycle/sec. Interrupted	4	25	.846	.831	.821	.824	-25	-7
Metal Electrodes, Pt-Pd Catalyzed	"	6	10	.906	.928	.849	.849	-57	-79

metal electrodes did not, in general, maintain constant cell voltages. The experimental conditions are tabulated in the left-hand columns and the changes in potential between the initial and final test day for the control and test cells are given in the far right-hand columns. For 1/4-inch carbon electrodes the average voltage changes agreed within 1 millivolt. For thin, composite electrodes the voltage changes for the pulsed electrodes average 20 mv lower than for the control cells. This observed difference, however, is still within the standard deviation of test results, indicating that this type of electrical pulsing had no significant effect.

Metal electrodes were subjected to short-term interrupted d. c. testing by maintaining the cell at constant current while scanning the frequency in the sonic range (circuit shown in Fig. 21). The results of these experiments at two current levels are shown in Fig. 26. Here it can be seen that the frequency of the interrupted d. c. had no significant effect on the cell voltage.

In experiments involving a. c. superimposed on d. c. for 1/4-inch carbon electrodes, the cell voltage held constant at 0.873 volt (IR-free) at currents of 50 ma d. c., 10 ma a. c.; and 50 ma d. c., 25 ma a. c.; while the frequency of the a. c. component was varied from 20 to 20,000 cps. At 100 ma d. c., 10 ma a. c. and 100 ma d. c., 25 ma a. c. the voltage held at 0.782 (IR-free) while the frequency of the a. c. component was varied over the same range. The experiments were repeated for IR-included potentials and these also did not vary even 1 mv over the frequency ranges noted above. Thin, composite and metal electrodes showed the same potential invariance with frequency. Even in cases where the peak value of the superimposed a. c. was greater than the d. c. level (e. g., 20 ma d. c., 50 ma a. c.), there were no clear effects on the cell voltage except small improvements due to heating caused by the capacitive current flow.

It was noted by K. V. Kordesch of our laboratory that in certain instances a short, heavy discharge pulse improved the performance level of electrodes significantly above that obtained by continuous discharge. The effect can best be described by reference to experimental data as shown in Fig. 27. The cell discharge current density is 75 ma/cm² and the heavy pulse current density is 350 ma/cm². The recorder here was set at zero center and 2000 mv full scale. Each cycle represents approximately 2 minutes,

including the 2-second heavy discharge pulse. At point "A" the cell voltage is 0.8 volt and decays to 0.76 volt under the 75 ma/cm² load after about two minutes (point "B"). The 2-second heavy discharge pulse drives the cell voltage to approximately -0.5 volt (point "C") after which the cell voltage recovers to 0.80 volt (point "D"), or 40 mv higher than before the heavy-pulse discharge. This phenomenon was observed over many hours with repetitious pulsing. The cell voltage later decreased to a failure point when left on continuous load.

In Figure 28, an even greater effect of heavy discharge pulsing is shown on another cell. After the 1-second heavy discharge pulse (500 ma/cm²) the cell voltage recovered 100 mv higher than it left off with (normal load 150 ma/cm², recorder set at 1000 mv full scale). At point "A" the normal discharge was continued for two hours without heavy discharge pulsing. The cell voltage decreased to 0.53 volt then recovered to an average of 0.68 volt when pulsing was resumed. Figure 29 pictures several hours of data from the same cell run at 100 ma/cm² and maintained at an average potential of 0.76 volt by heavy discharge pulsing. The recorder paper speed is 2 inches/hour.

Preliminary results obtained on Pd, Pt, and Rh catalyzed composite electrodes showing improvements are summarized in Table III. The pulse repetition rate was one pulse every three minutes (except where specified).

TABLE III
HEAVY DISCHARGE PULSING DATA FOR COMPOSITE ELECTRODES

Catalyst	Electrode	Current Density (ma/cm ²)	Polarization(mv)		Duration (sec.)	Pulse Intensity	
			Before Pulse	After Pulse		C. D. (ma/cm ²)	Polarization
Pd	Anode	20	122	103	1.0	900	1006
Pd	Anode	30	168	157	1.0	900	1016
Pd	Cathode	50	70	60	2.5	2000	250
Pd	Cathode	100	80	70	2.5	2000	250
Pt	Anode*	25	230	212	1.0	500	1400
Pt	Anode	25	350	284	1.0	400	1400
Pt	Cathode	25	50	40	1.0	2000	260
Rh	Cathode**	25	22	17	2.5	2000	455

* Anode was left on steady current and allowed to deteriorate to the specified polarization before applying pulse.

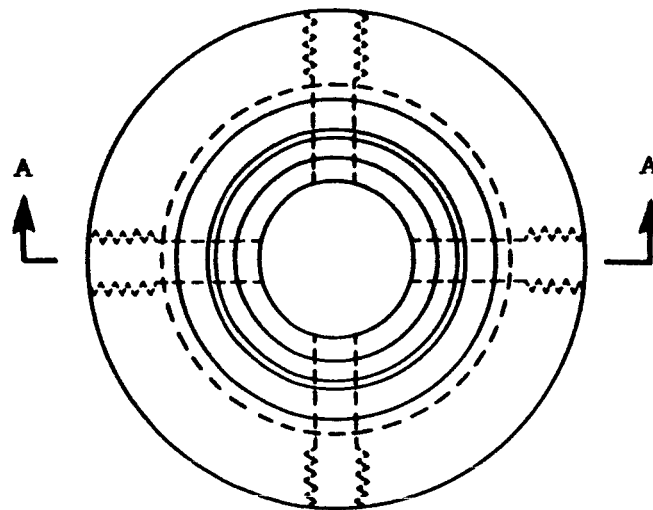
** No improvement was noted on rhodium catalyzed anodes as a result of pulsing in two series of experiments.

The fourth main column giving the electrode polarization (OCV as reference) before and after the applied pulse indicates the extent of the improvement that resulted from the applied pulse. The intensity of the pulse expressed in terms of current density and electrode polarization is given in the far-right column.

From Table III, on the basis of this preliminary data it may be concluded that electrical pulsing affects differently catalyzed electrodes in a different way.

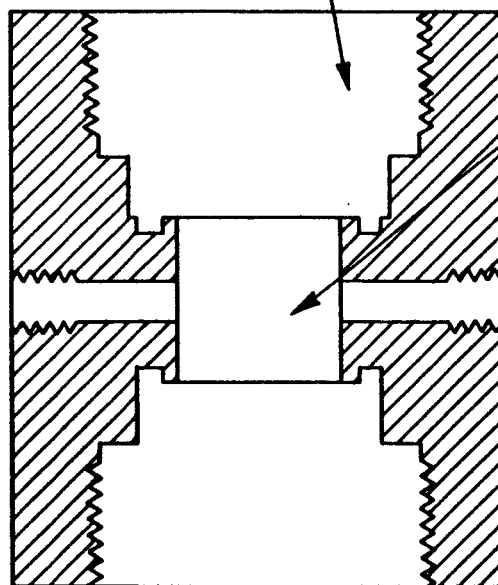
It is believed that improvements resulting from heavy discharge pulsing may be related to catalyst reactivation. Heavy discharge pulsing will continue to be investigated.

APPENDIX



Front View

Electrode and Gas Room

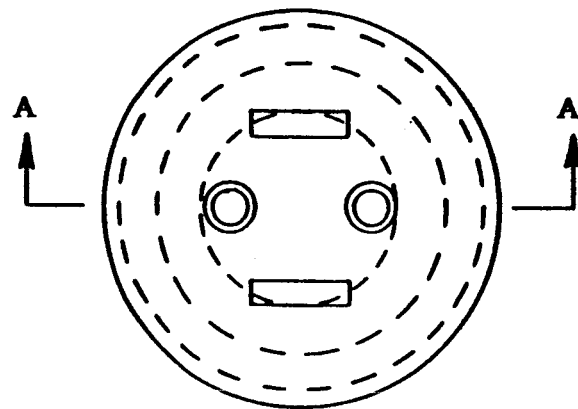


Electrolyte Room

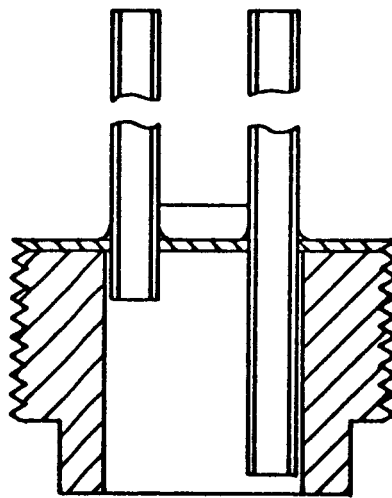
Section AA

D-472

Fig. 1 Drawing of Teflon Cell Used for Electrolyte and Gas Pulsing.



Front View



Section AA

D-473

Fig. 2 Drawing of Stainless Steel Electrode Holder and Gas Chamber.

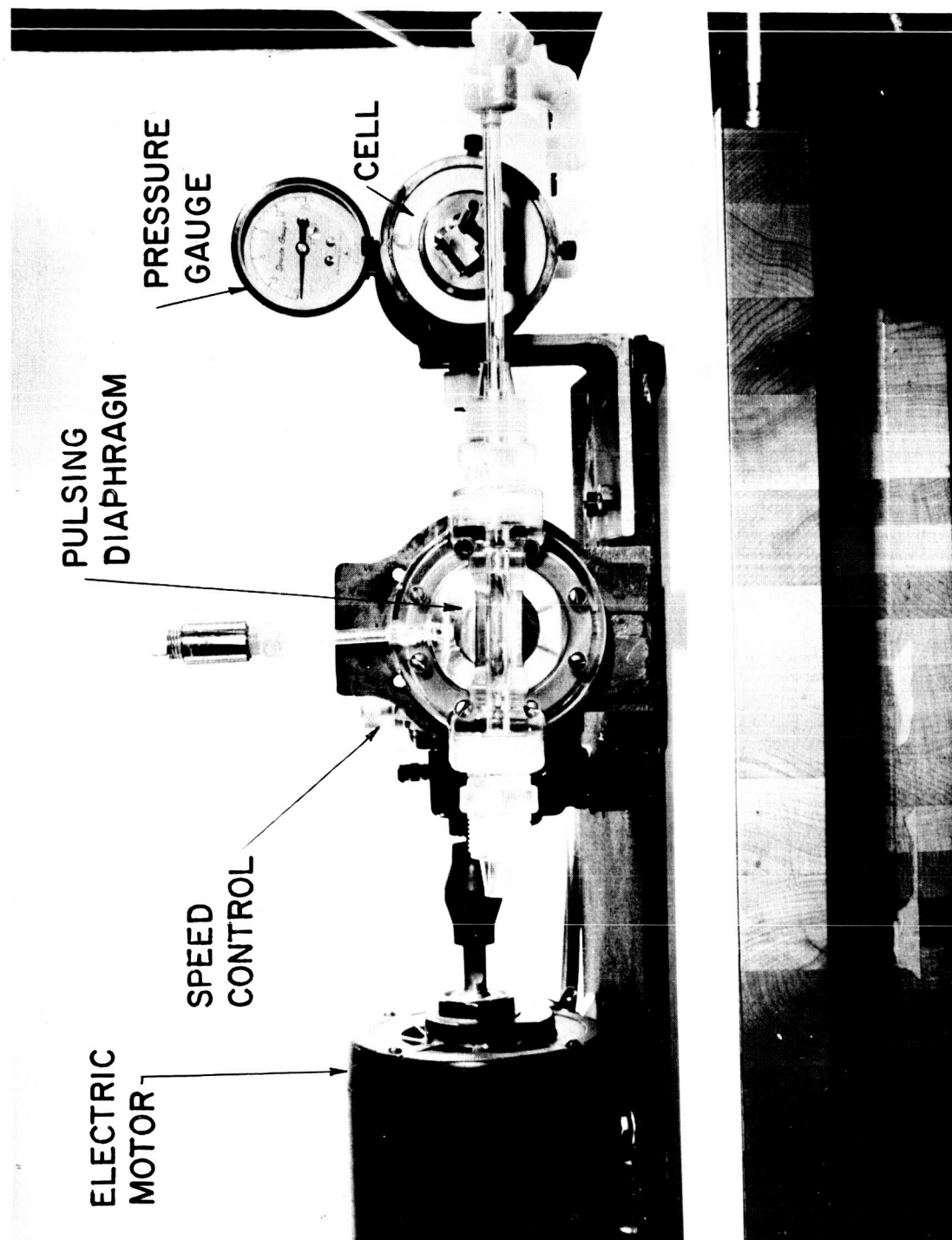


Fig. 3 System for Subsonic Gas and Electrolyte Pulsing

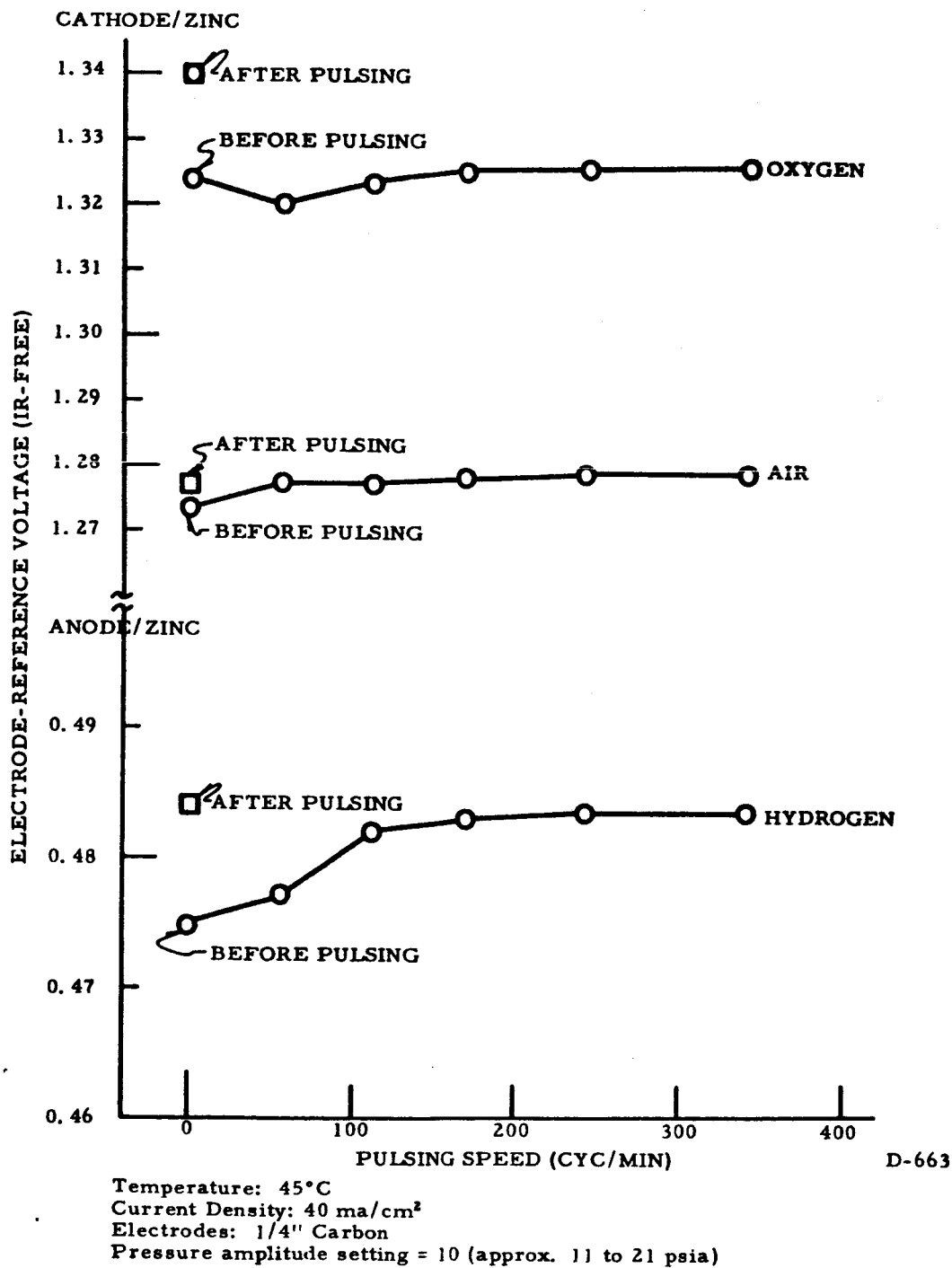


Fig. 4 Electrode-Reference Potential as a Function of Pulsing Speed.

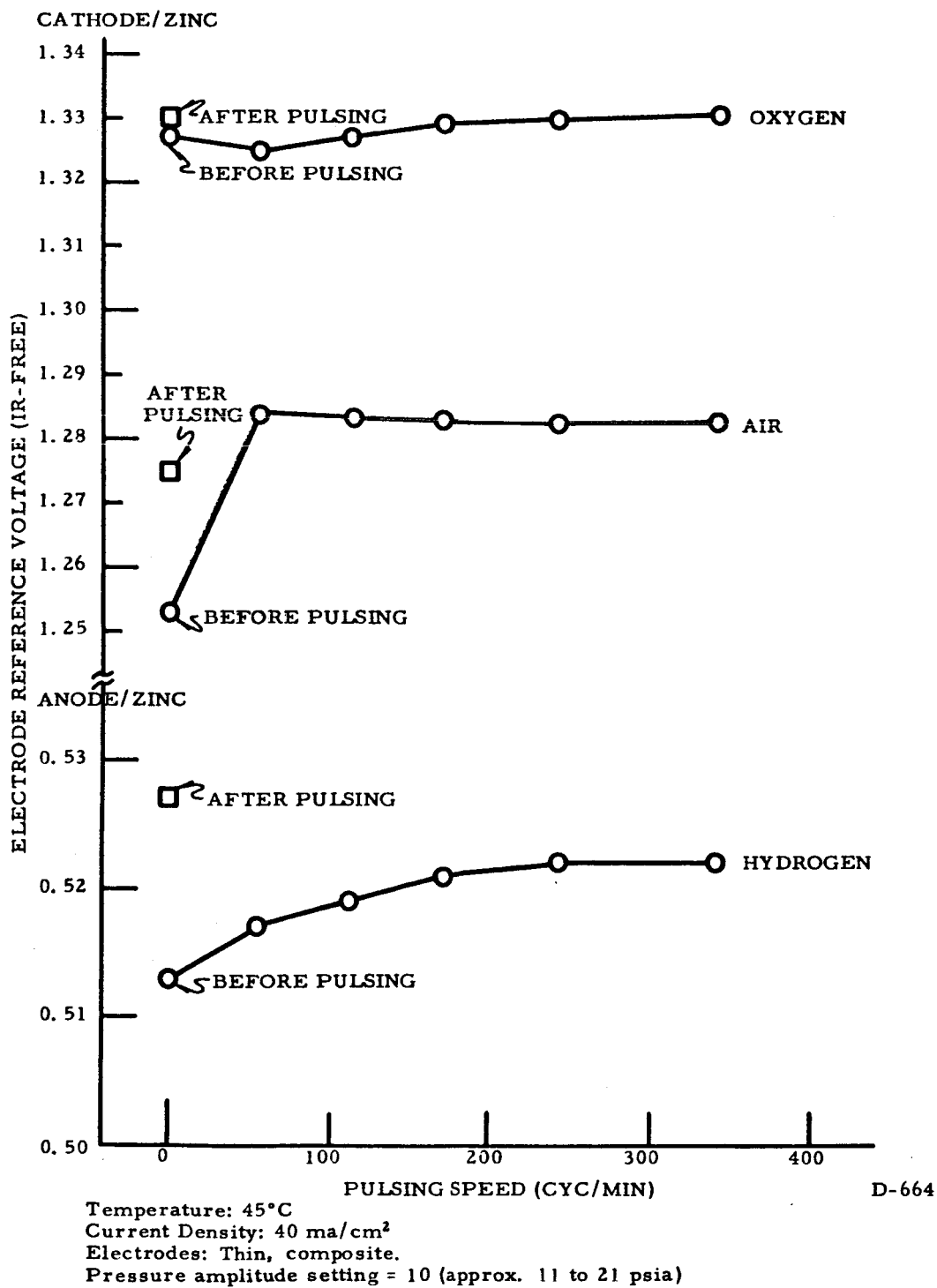
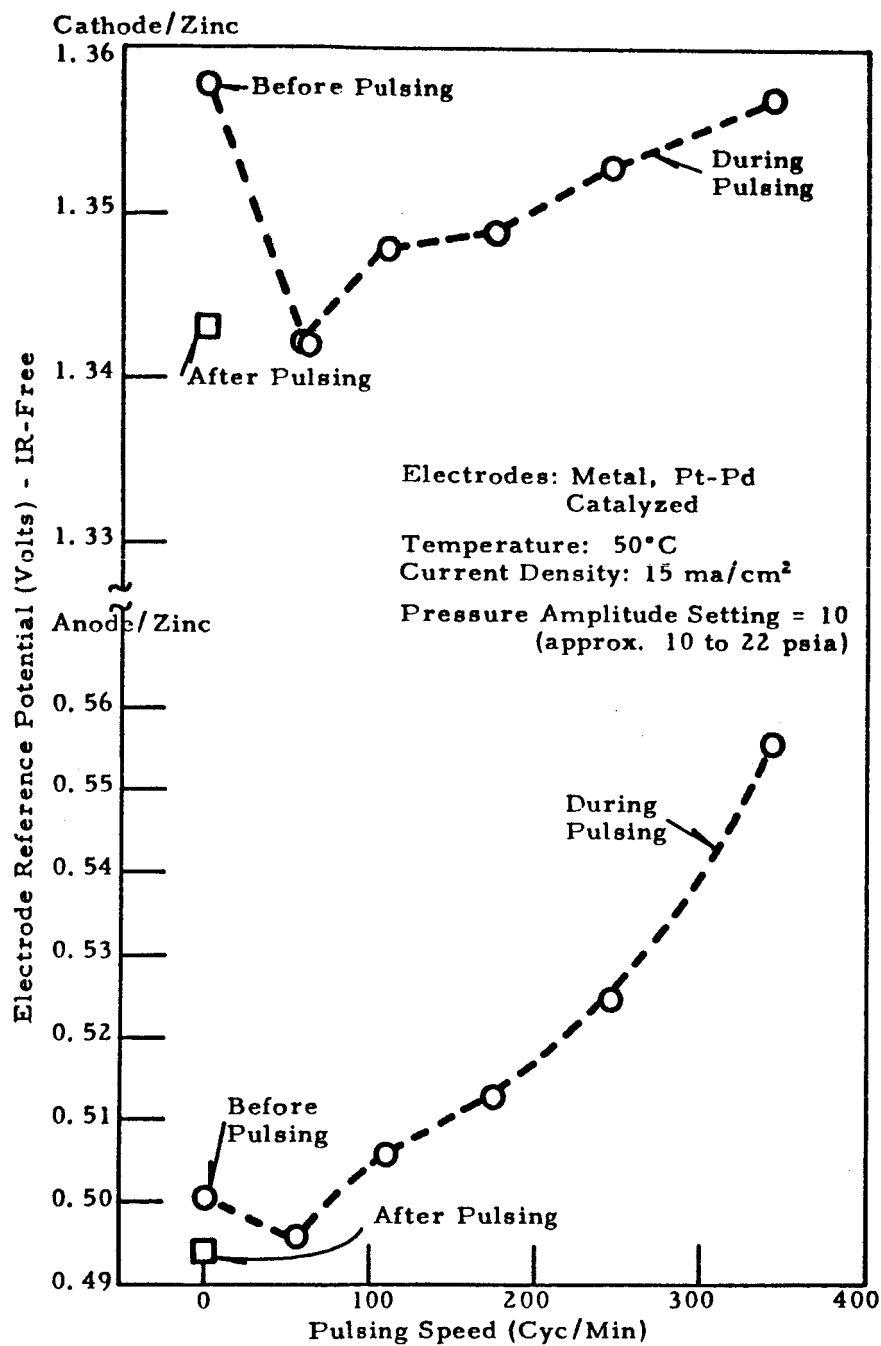


Fig. 5 Electrode-Reference Potential as a Function of Pulsing Speed.



D-1155

Fig. 6 Electrode-Reference Potentials as a Function of Pulsing Speed

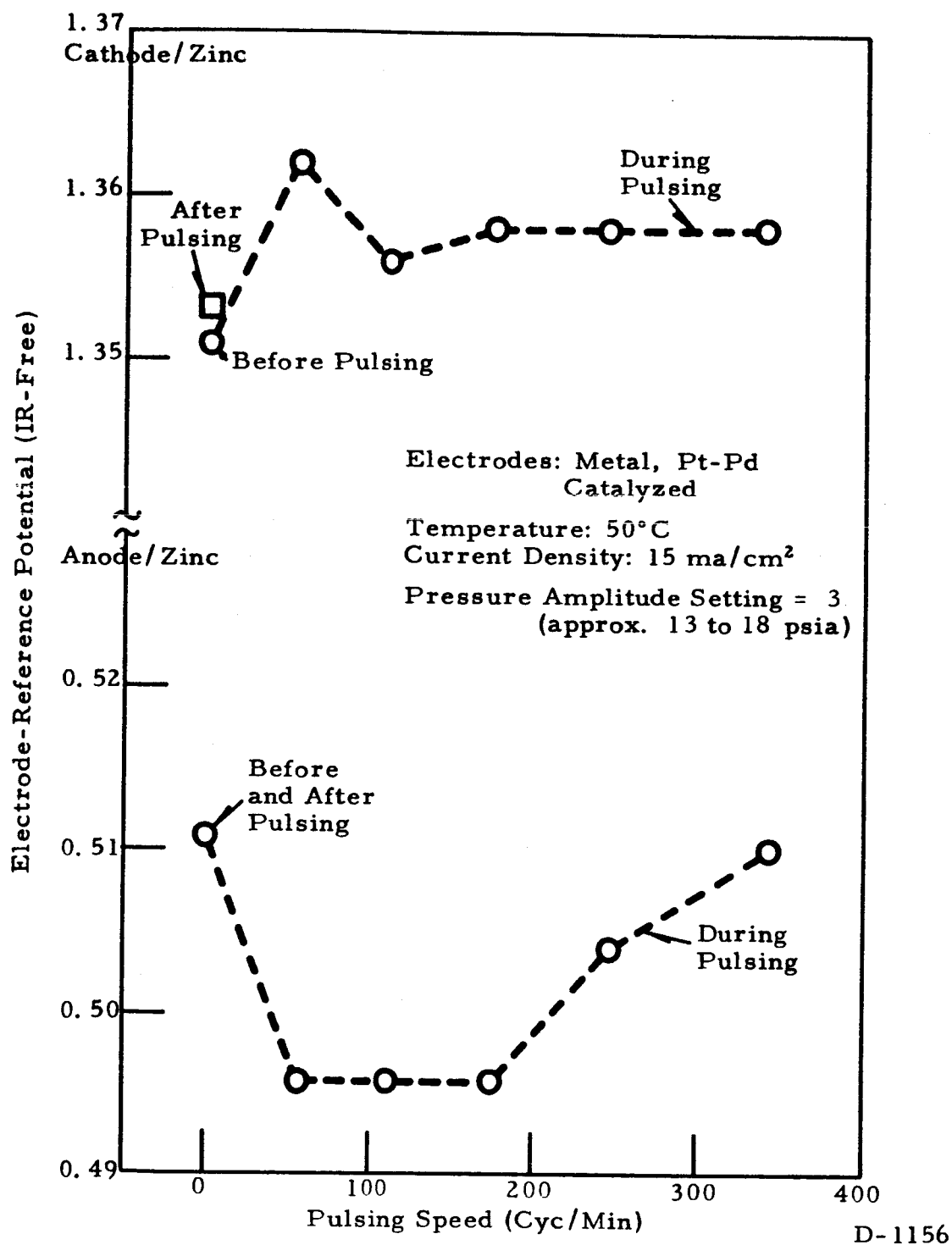
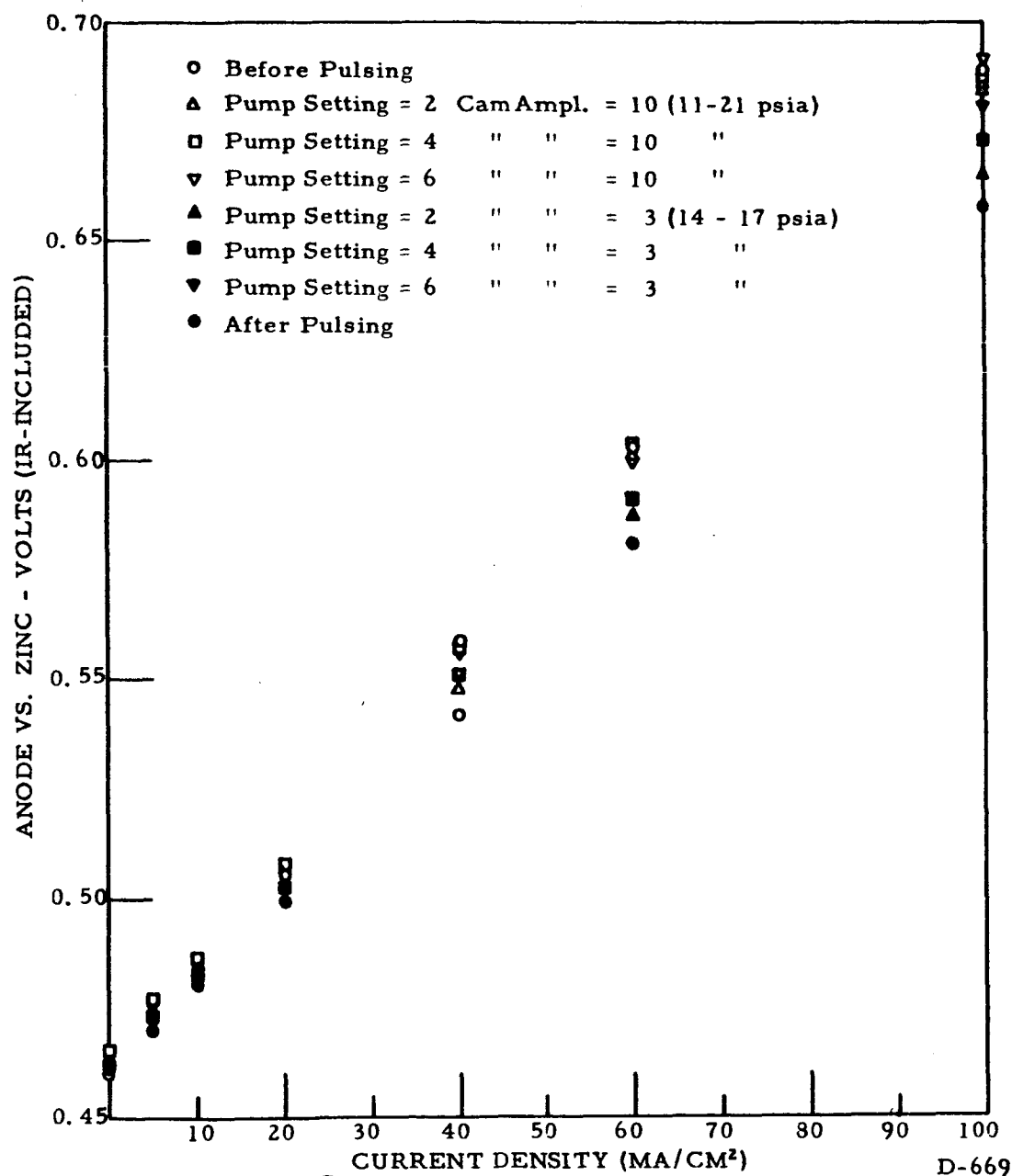
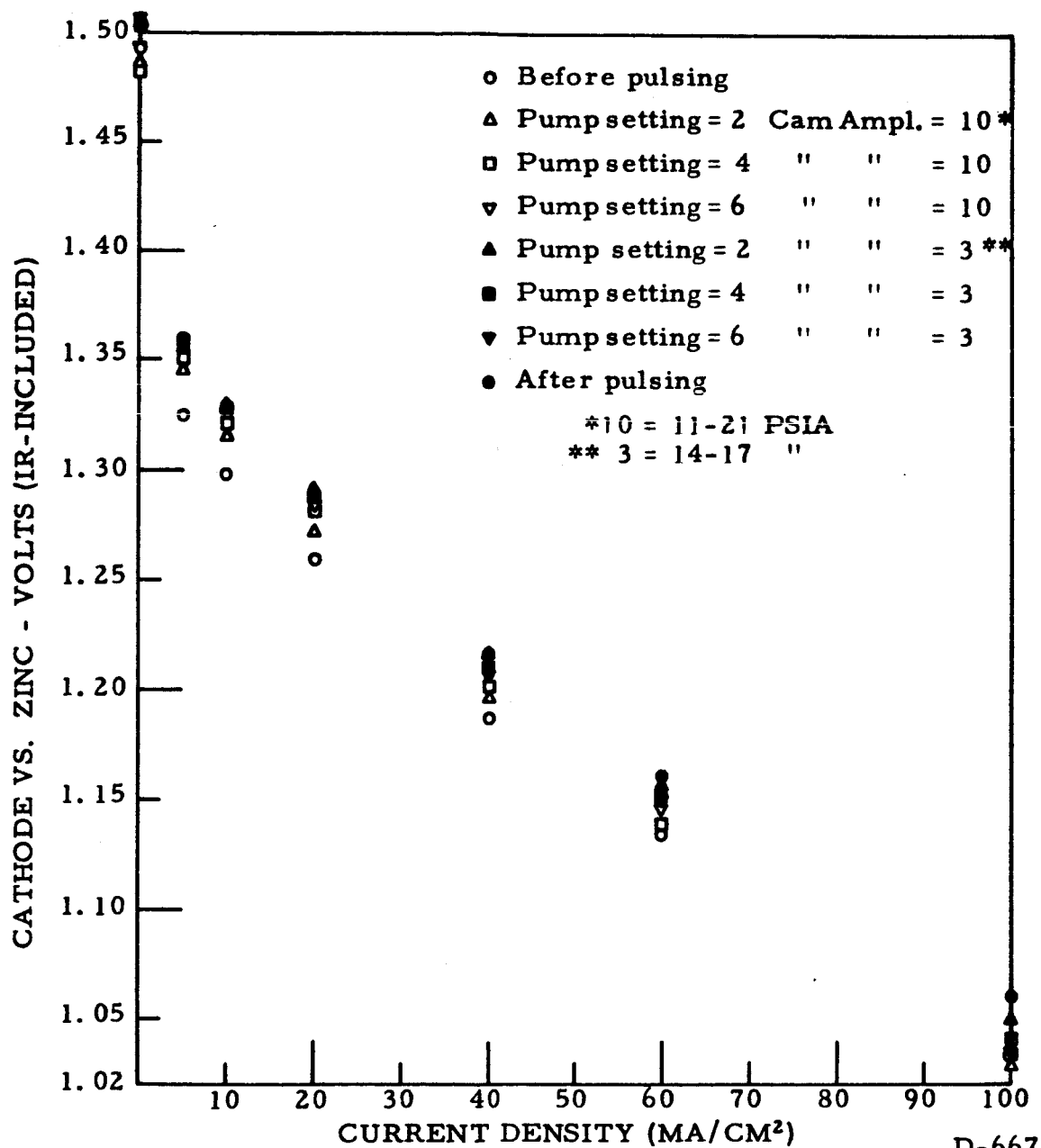


Fig. 7 Electrode-Reference Potentials as a Function of Pulsing Speed



Temperature: 45°C
 Electrodes: 1/4" Carbon
 Anode Fuel Gas: Hydrogen

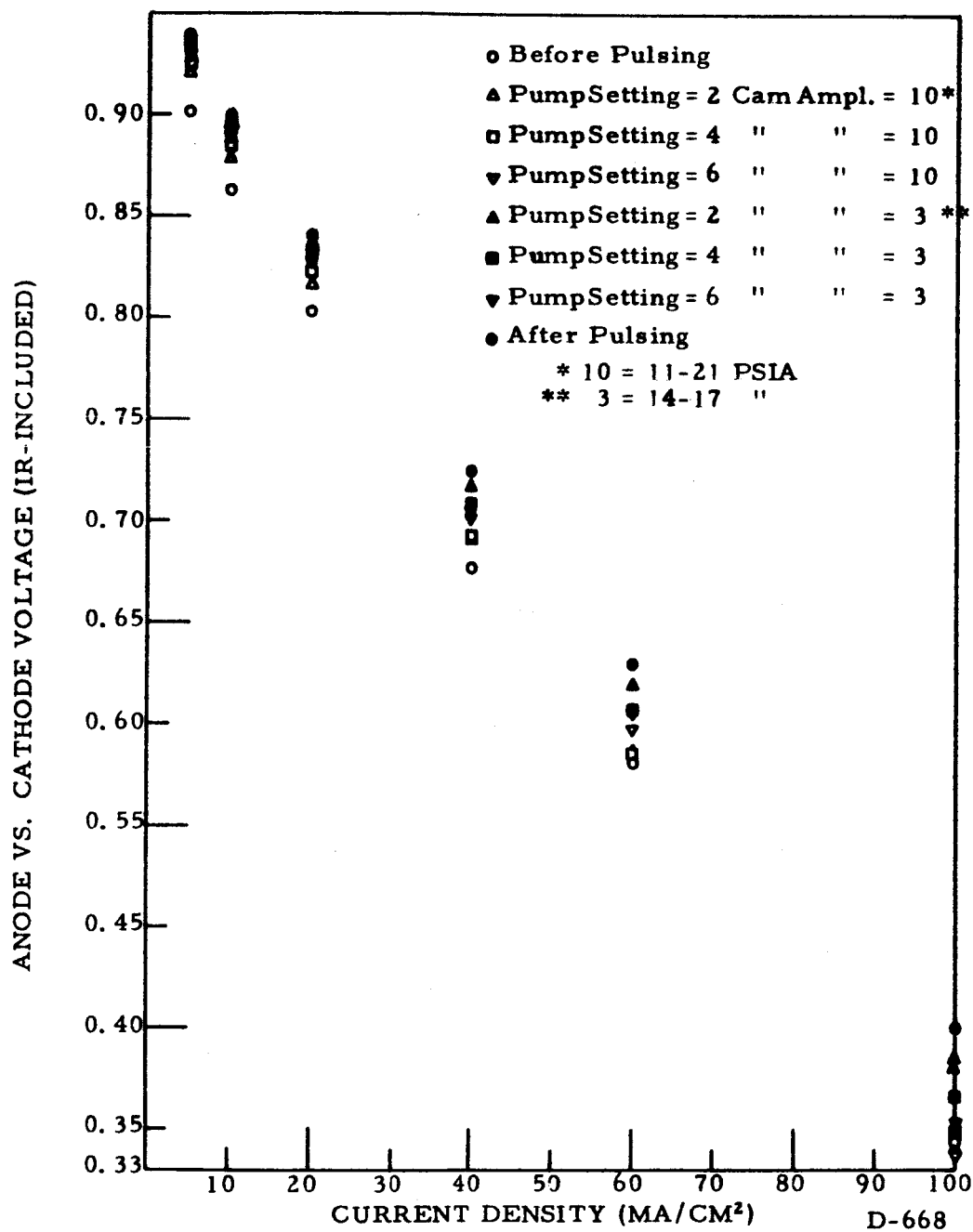
Fig. 8 Anode-Reference Polarization Curves; Before, During and After Pulsing.



Temperature: 45°C
Electrodes: 1/4" Carbon
Cathode Fuel Gas: Oxygen

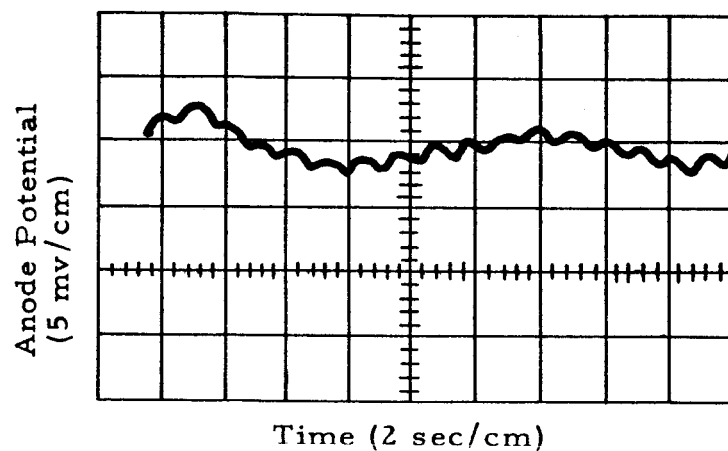
D-667

Fig. 9 Cathode-Reference Polarization Curves; Before, During and After Pulsing.



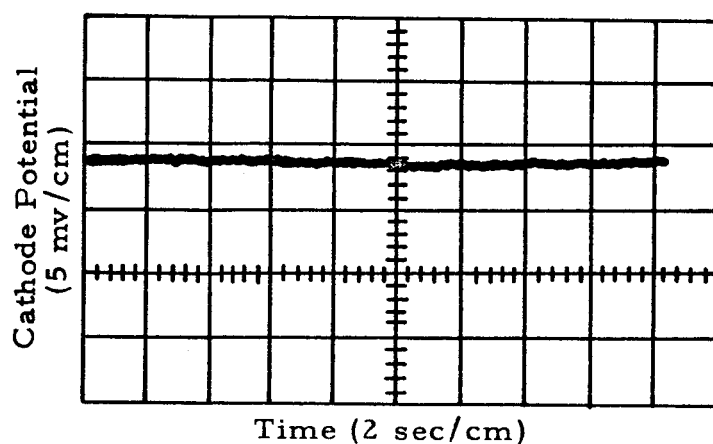
Temperature: 45°C
 Electrodes: 1/4" Carbon
 Anode Fuel Gas: Hydrogen
 Cathode Fuel Gas: Oxygen

Fig. 10 Anode-Cathode Polarization Curves; Before, During and After Pulsing.



D-1157

Fig. 11 Oscilloscope Trace of Anode-Reference Potential Fluctuations During Mechanical Pulsing of Electrolyte.



D-1158

Fig. 12 Oscilloscope Trace of Cathode-Reference Potential Fluctuations During Mechanical Pulsing of Electrolyte.

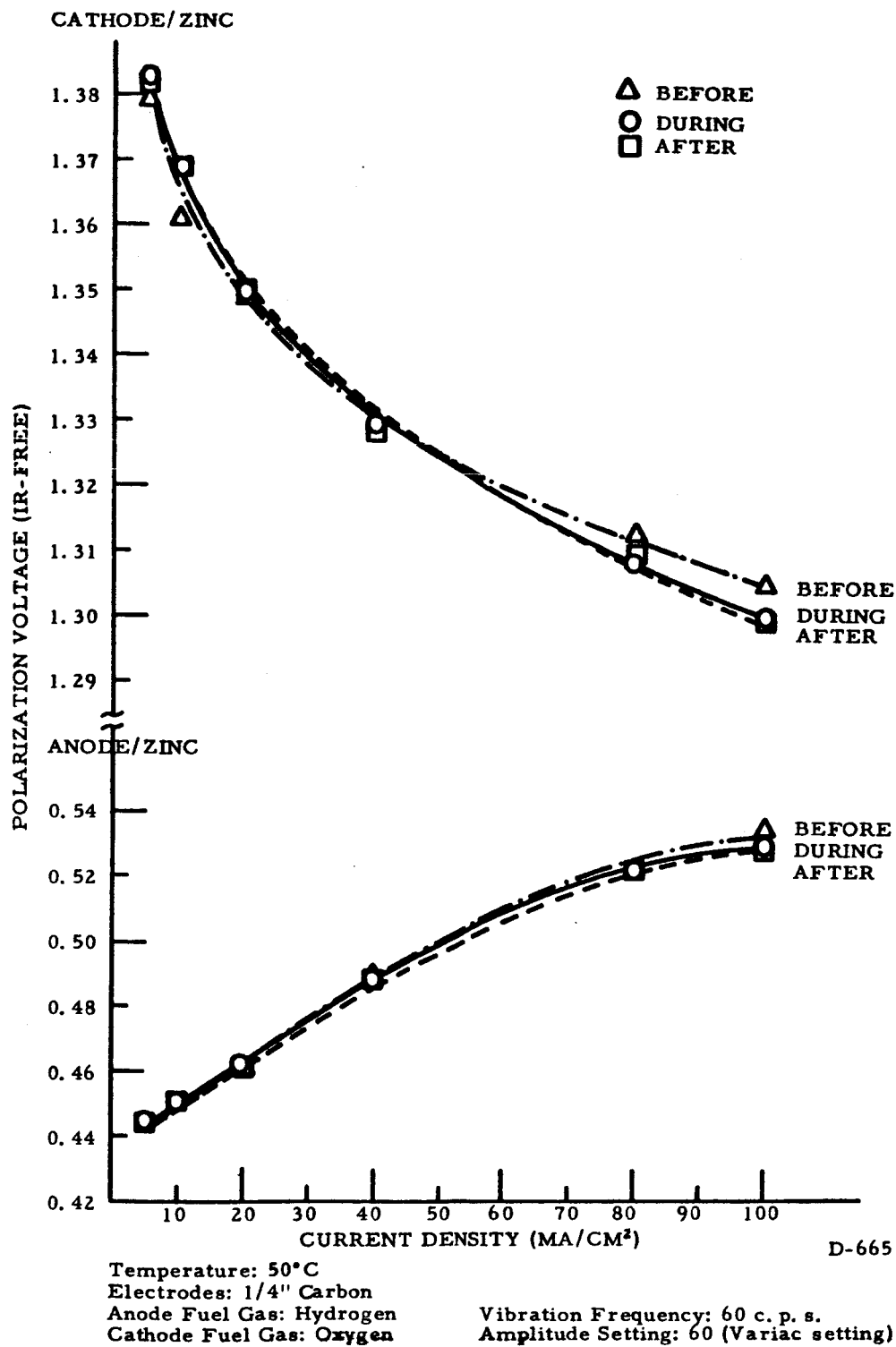


Fig. 13 Polarization Curves Before, During and After Vibration Tests.
 (IR-Free)

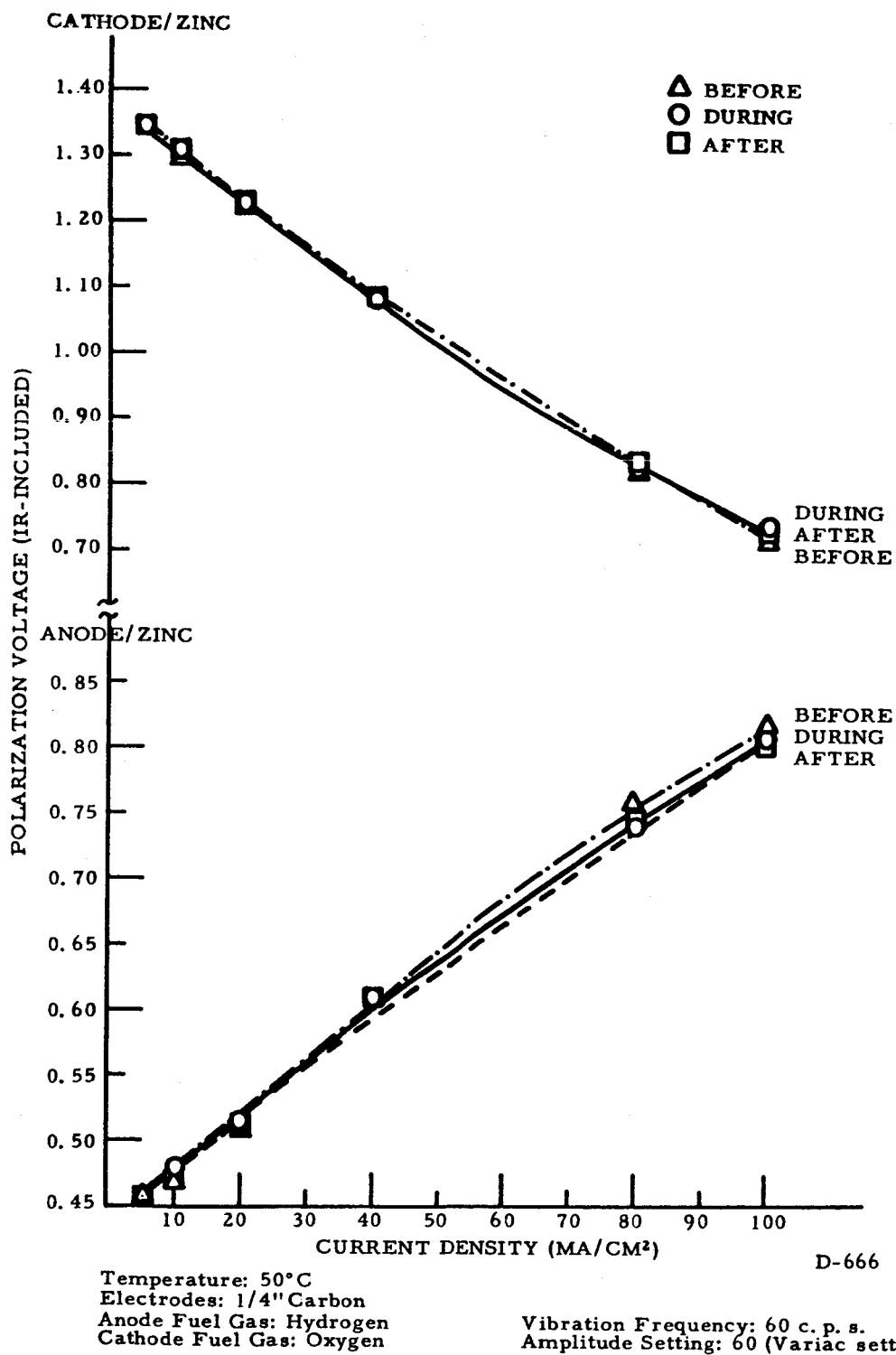
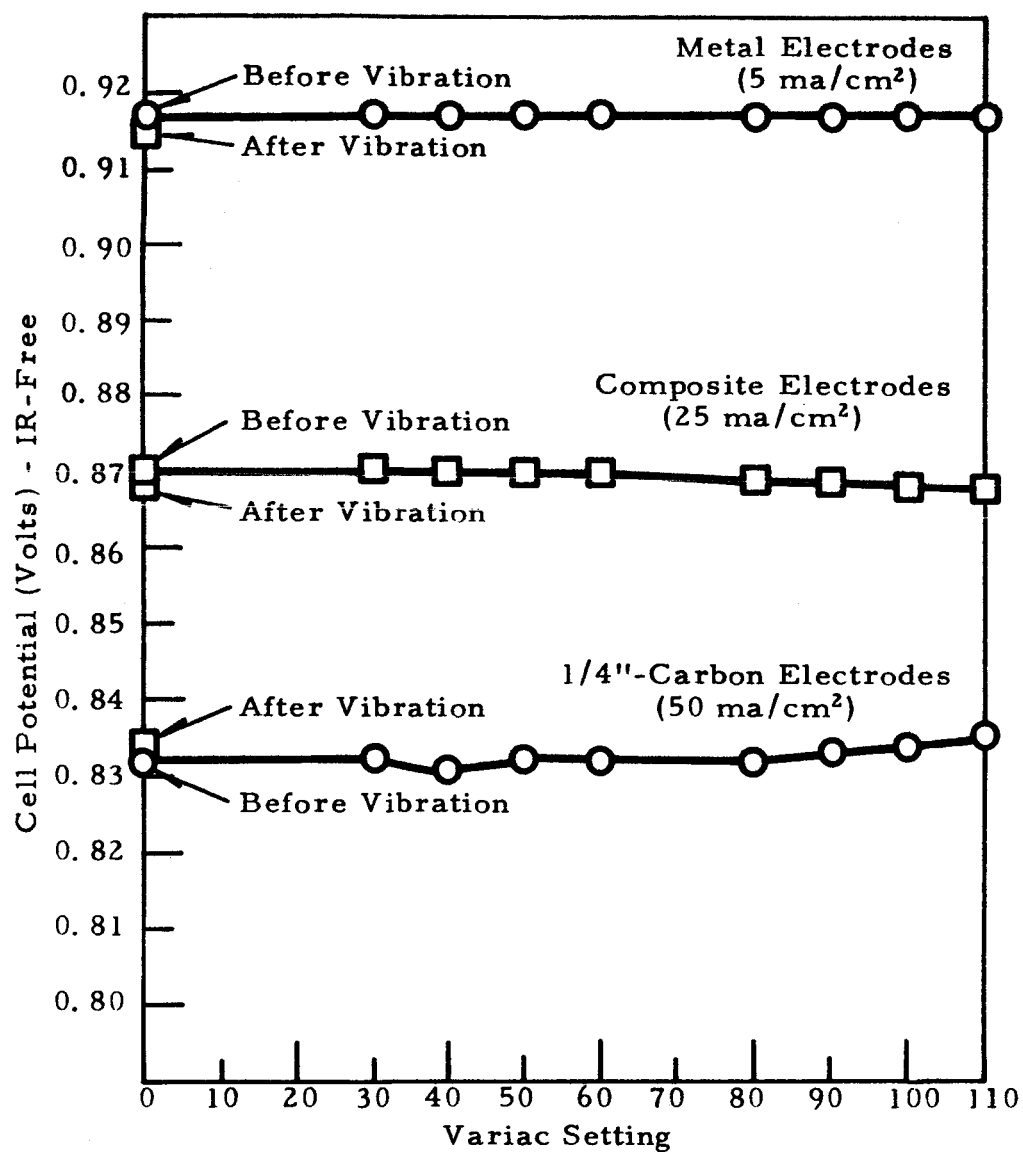
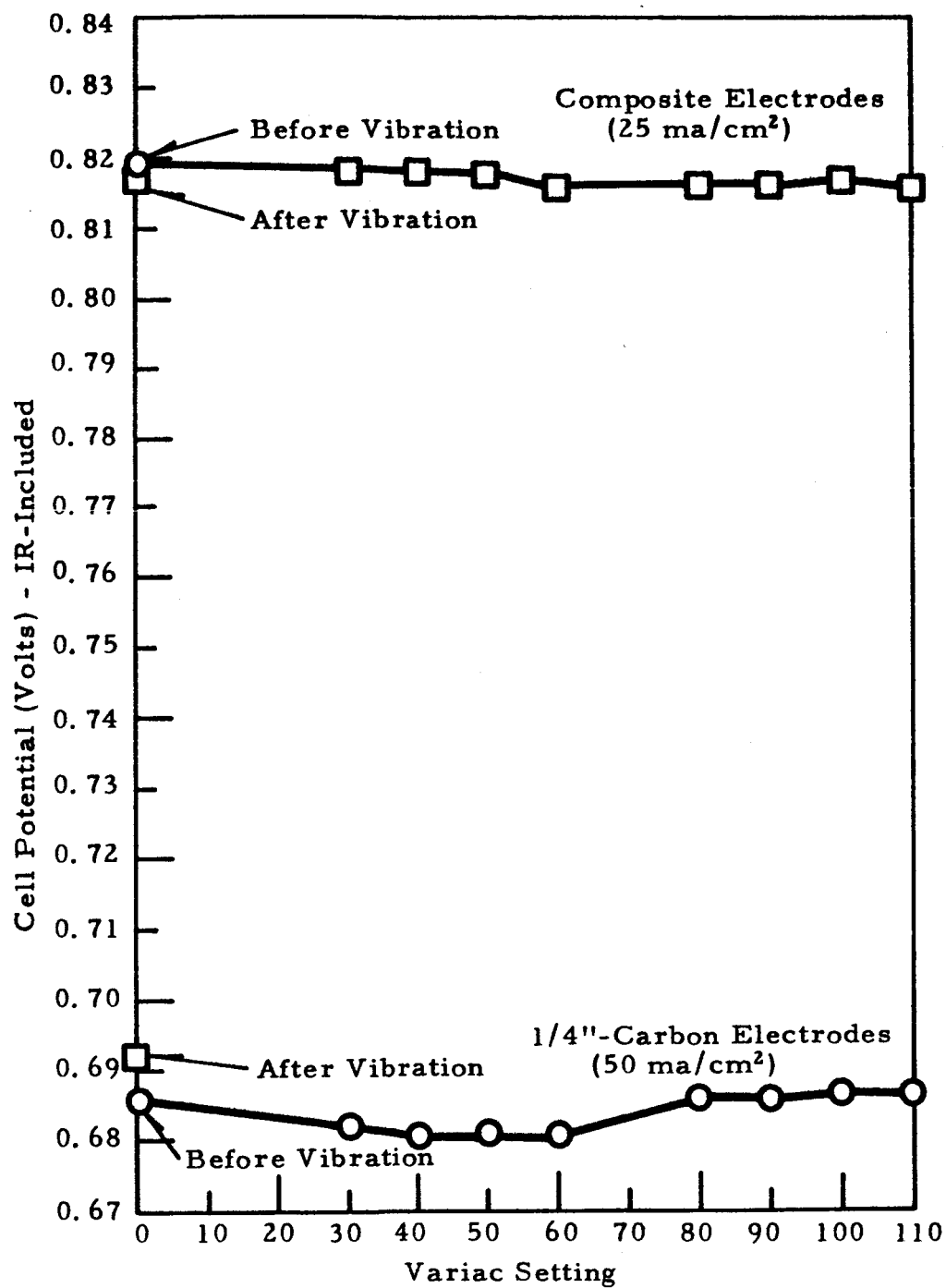


Fig. 14 Polarization Curves Before, During and After Vibration Tests.
(IR-Included)



D-1159

Fig. 15 IR-Free Cell Voltage vs. Vibration Amplitude at Constant Current and Constant Frequency of 60 Cycles/Second.



D-1160

Fig. 16 IR-Included Cell Voltage vs. Vibration Amplitude at Constant Current and Constant Frequency of 60 Cycles/Second.

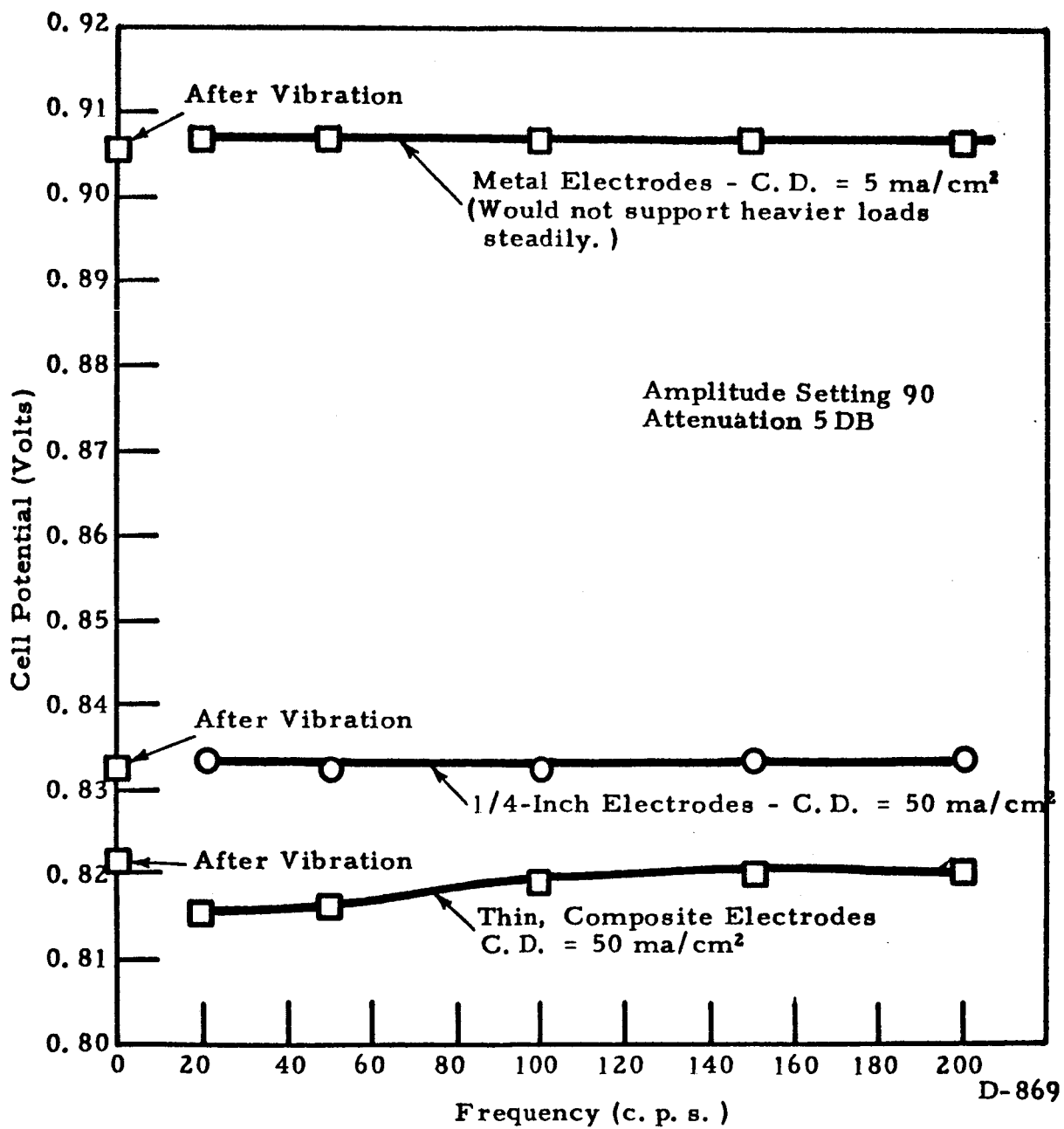
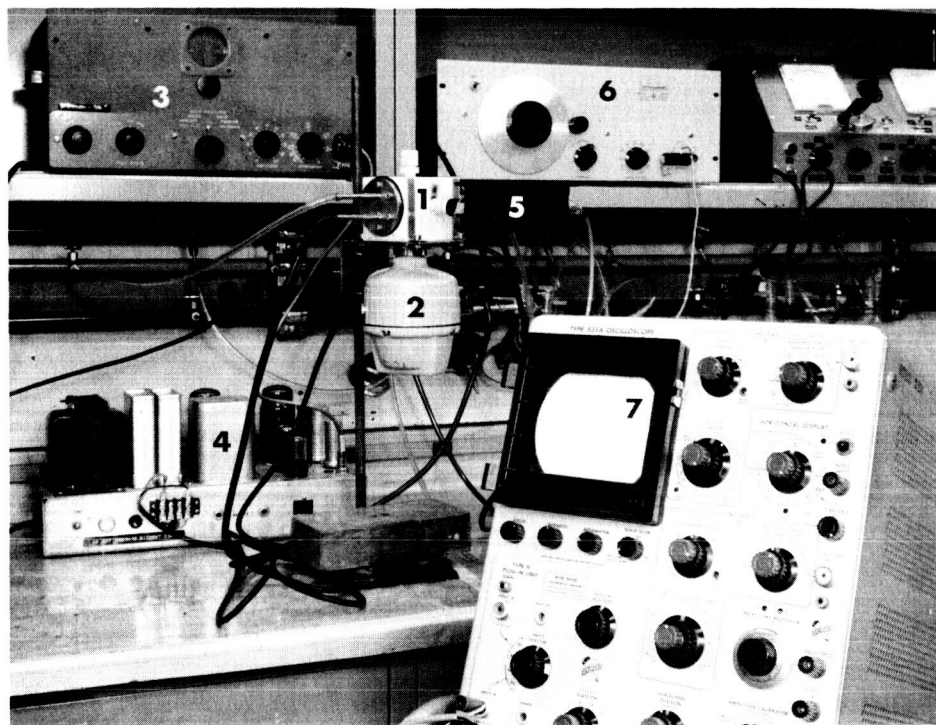


Fig. 17 Cell Voltage vs. Vibration Frequency
for Three Types of Electrodes.



D-791

Fig. 18 Equipment for Sonic Pulsing of Electrolyte

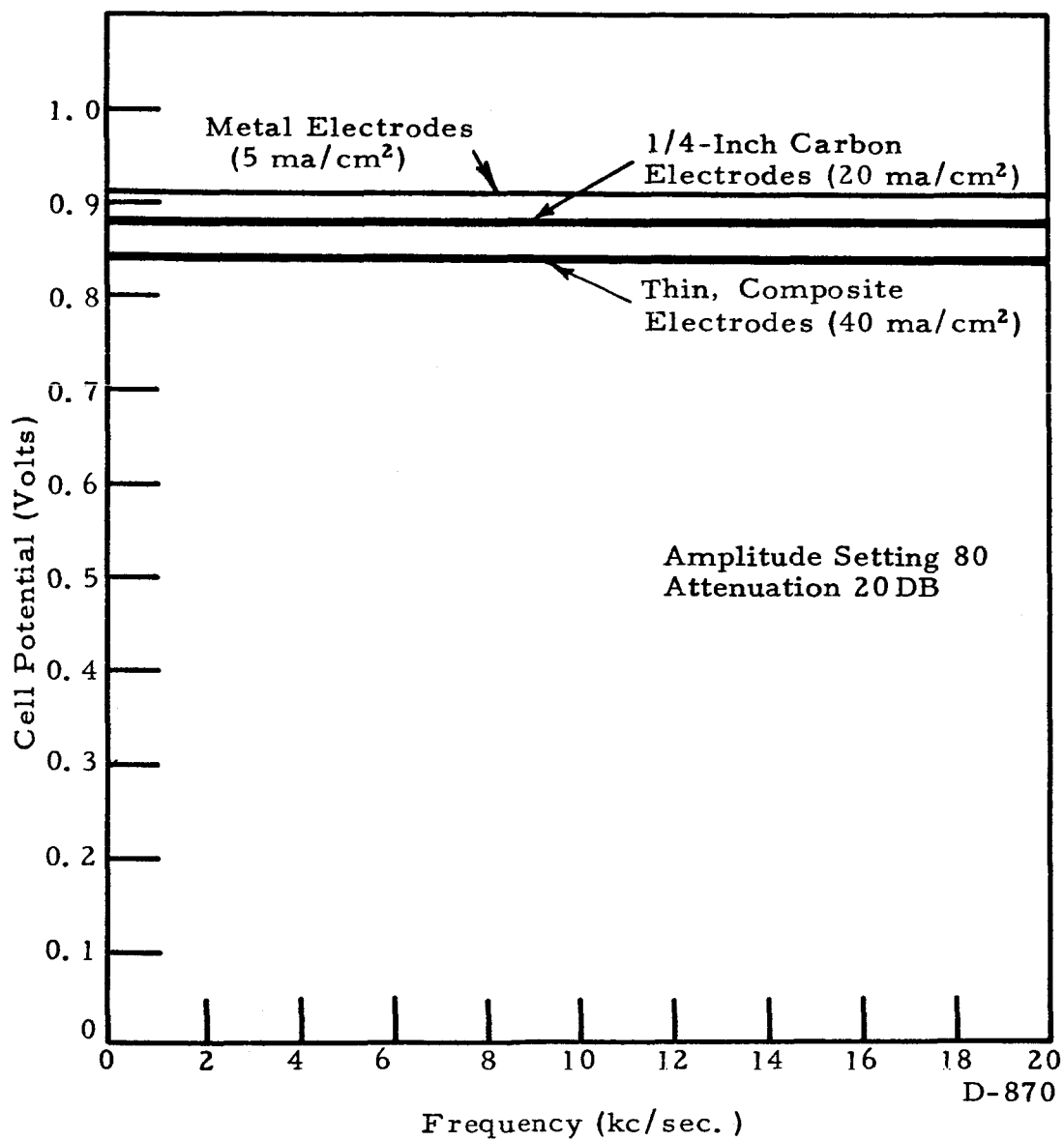
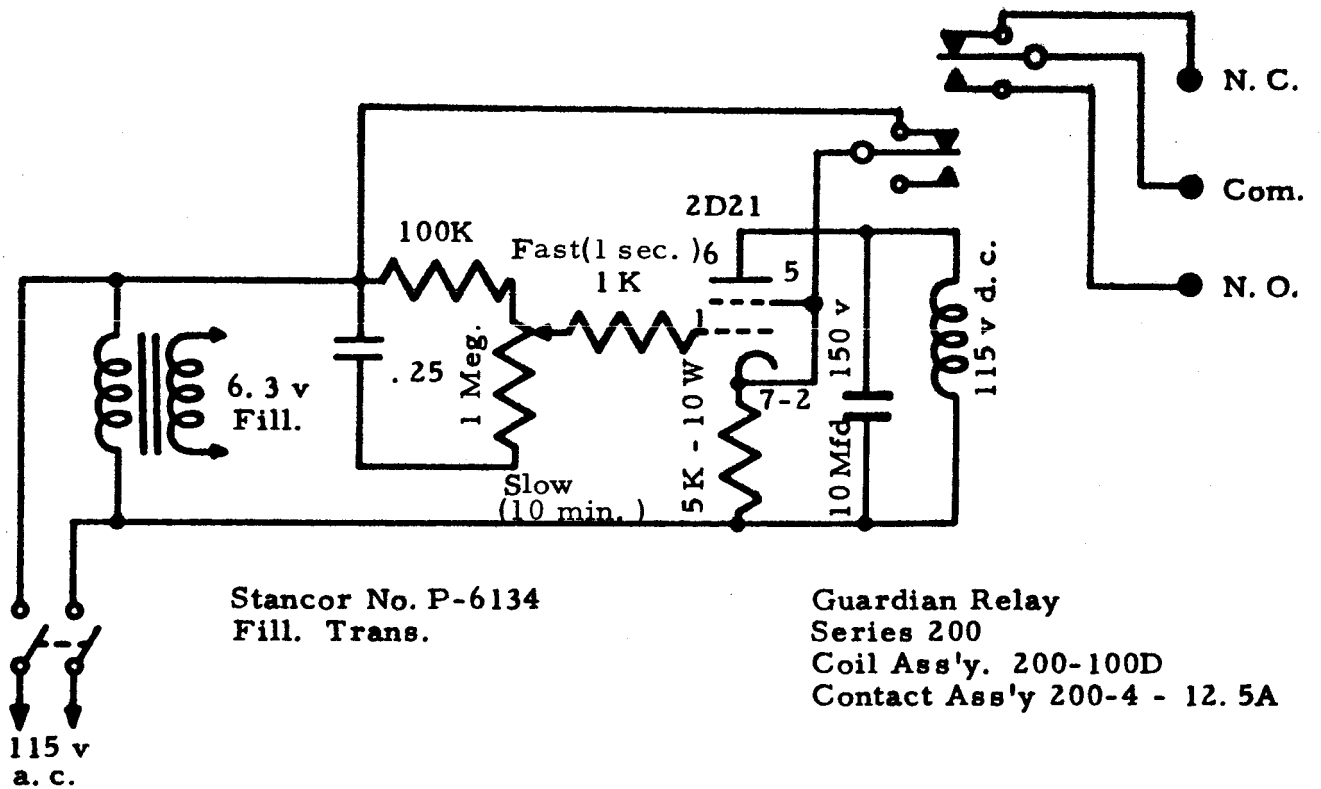


Fig. 19 Effect of Electrolyte Pulsations on Cell Voltage for Metal, 1/4-Inch Carbon, and Thin-Composite Electrodes



D-1162

Fig. 20 Variable Rate Timer Switch

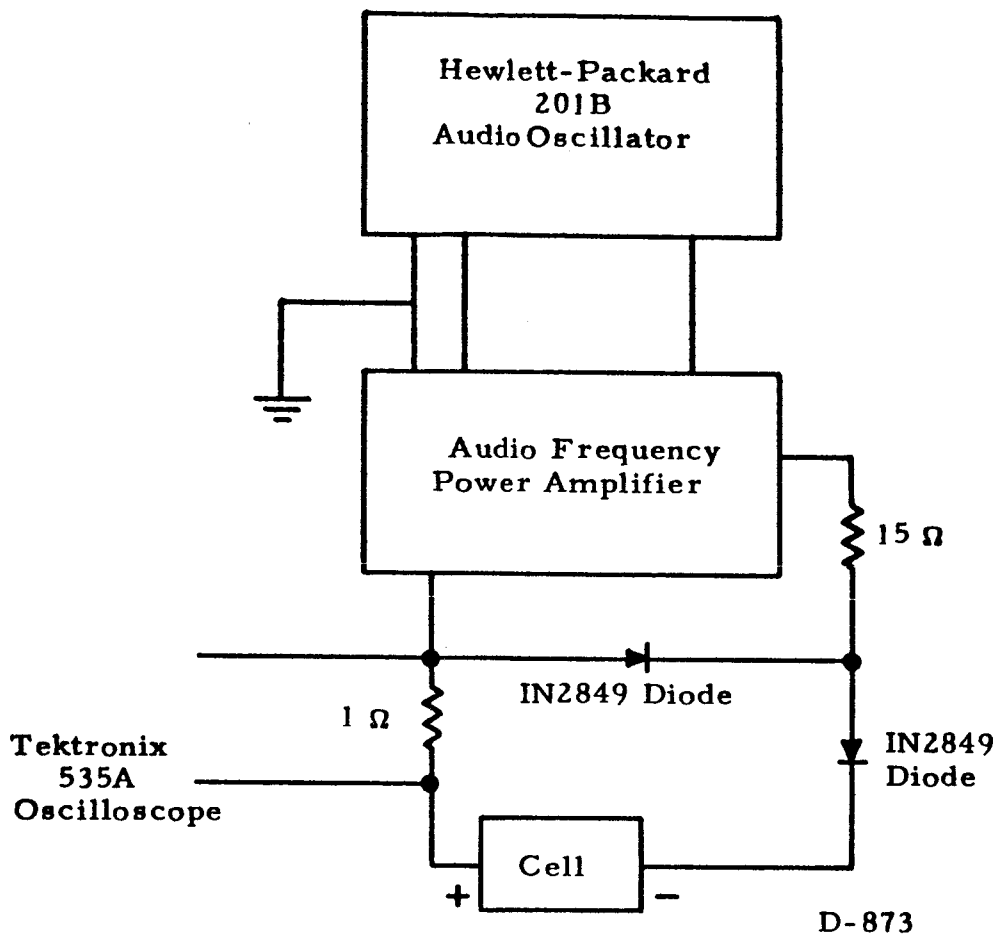
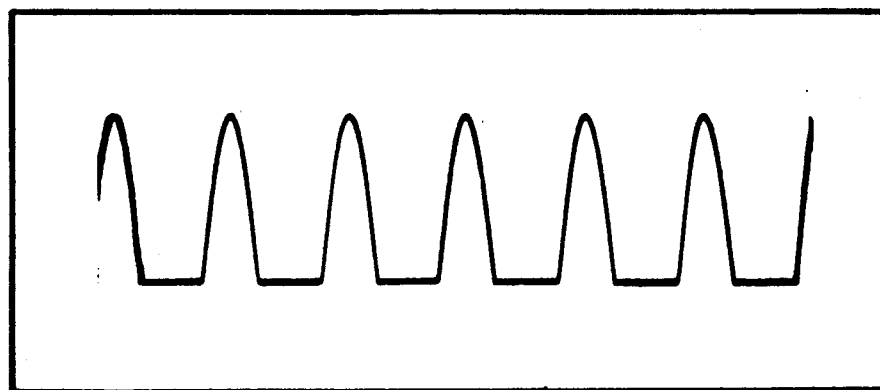
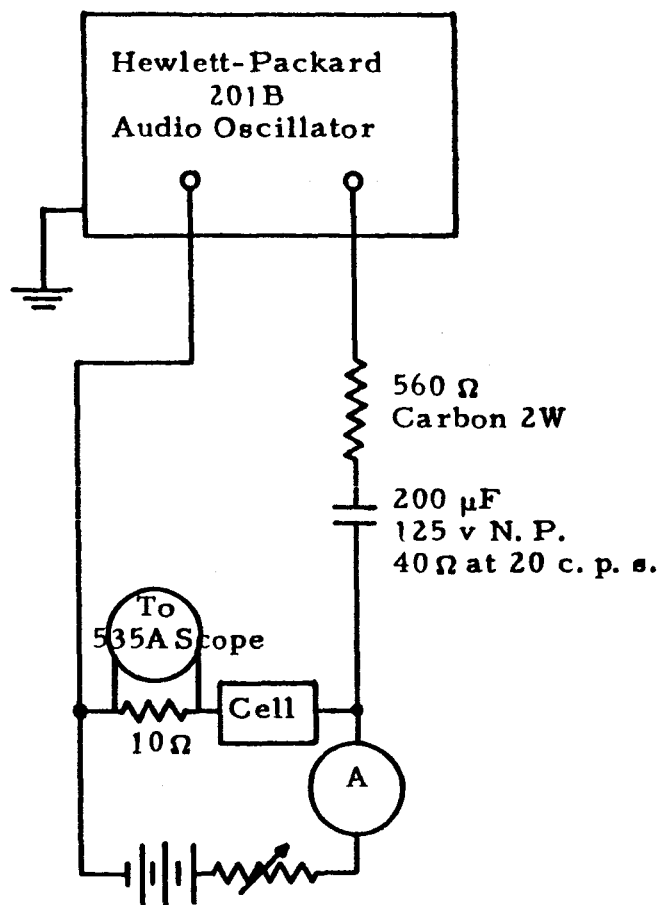


Fig. 21 Circuit Used for Interrupted D. C.



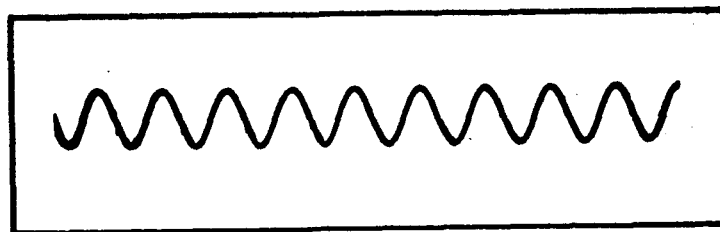
D-867

Fig. 22 Interrupted D. C. Wave Form.
(300 c. p. s. , Avg. Current 100 ma)



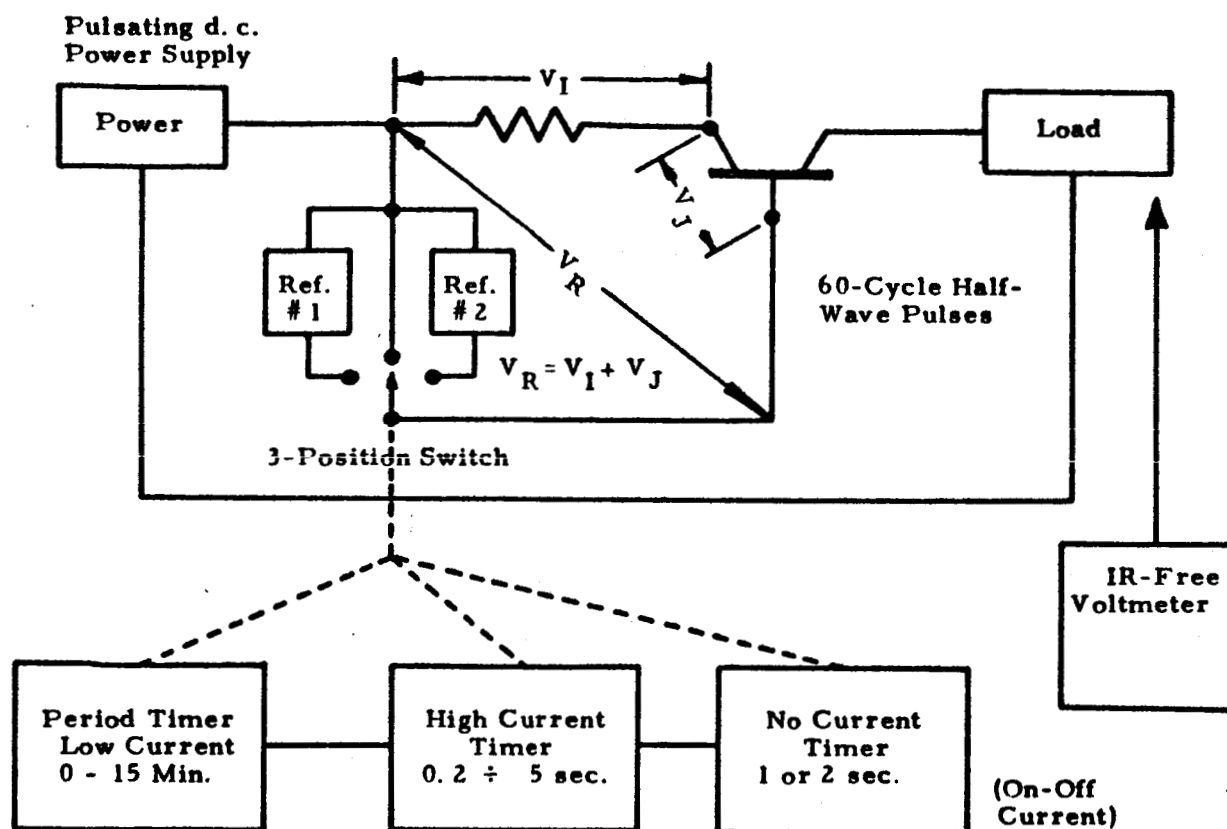
D-874

Fig. 23 Circuit Diagram for A. C. Superimposed on D. C.



D-868

Fig. 24 Wave Form of A. C. Superimposed on D. C. -
50 ma D. C. , 10 ma Superimposed A. C. -
(1000 c. p. s.) - 200 mv/cm.
Sweep Time = 1 millisc. /cm.



Note: Ref. # 1 - Voltage control for low current range.
 Ref. # 2 - Voltage control for high current range.

D-1163

Fig. 25 Dual Range Constant Current Interrupter. Timer Controlled.

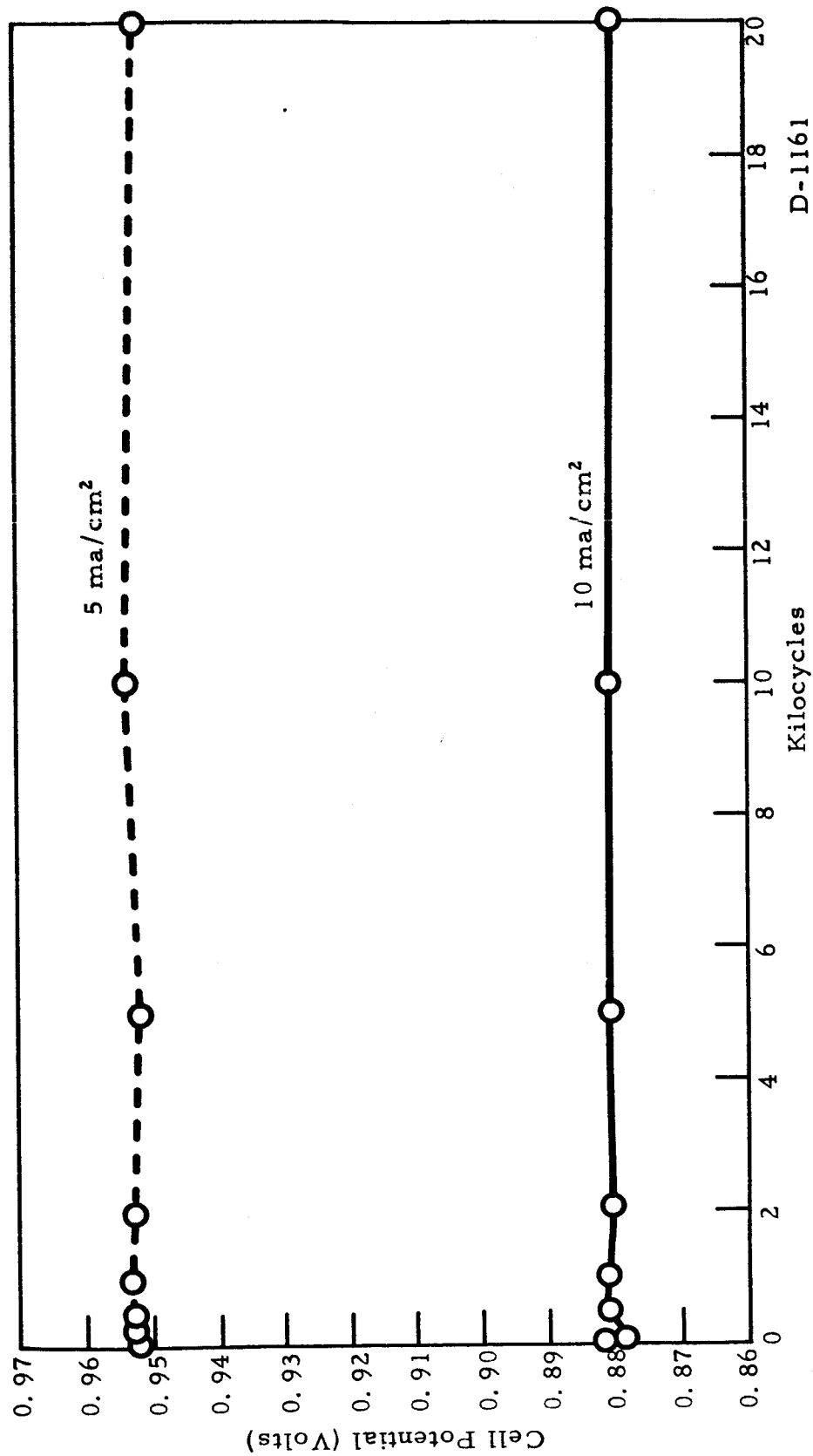


Fig. 26 Cell Voltage vs. Frequency of Interrupted d. c. for Metal Electrodes

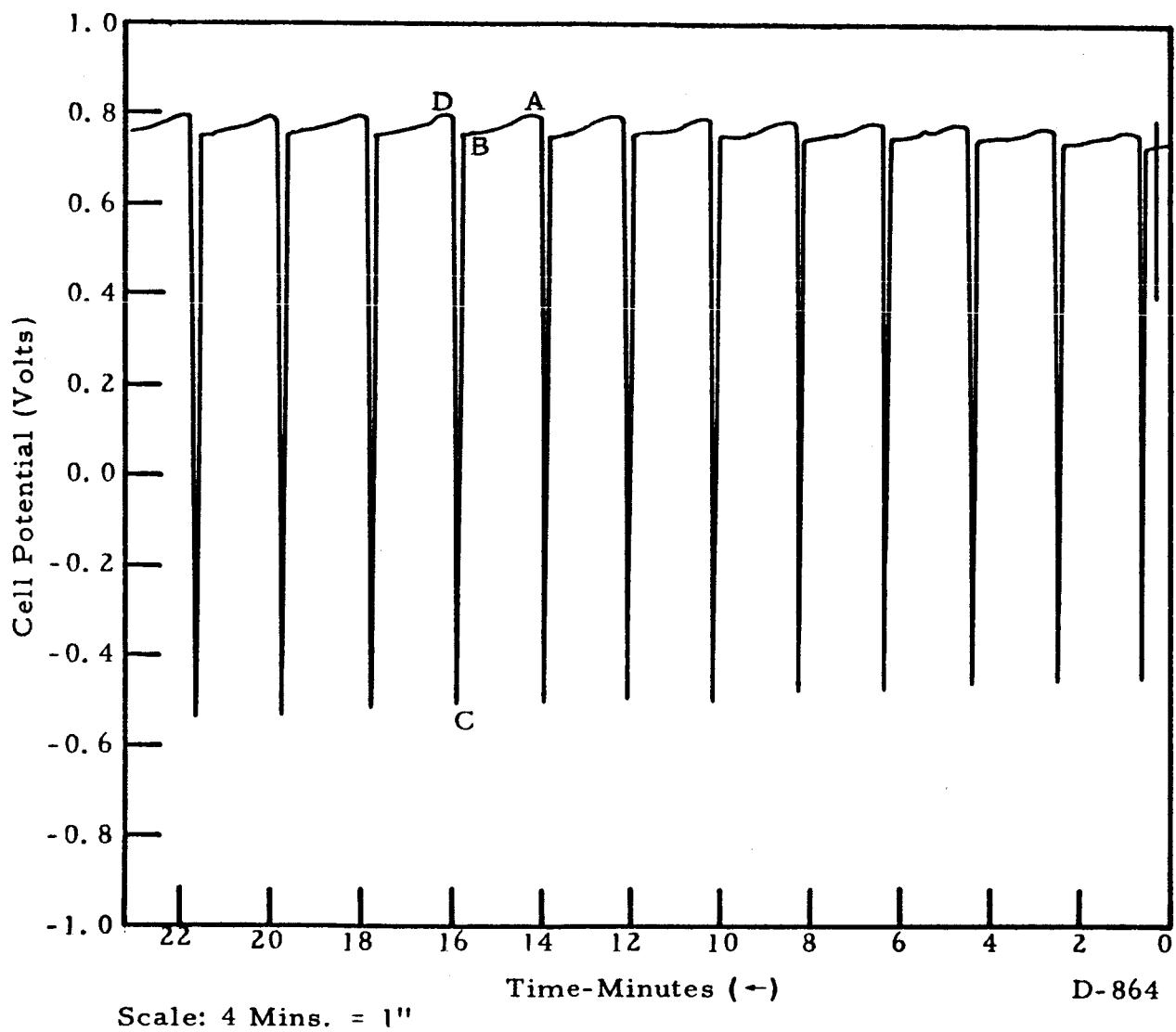


Fig. 27 Effect of Heavy Discharge Pulse on Cell Voltage

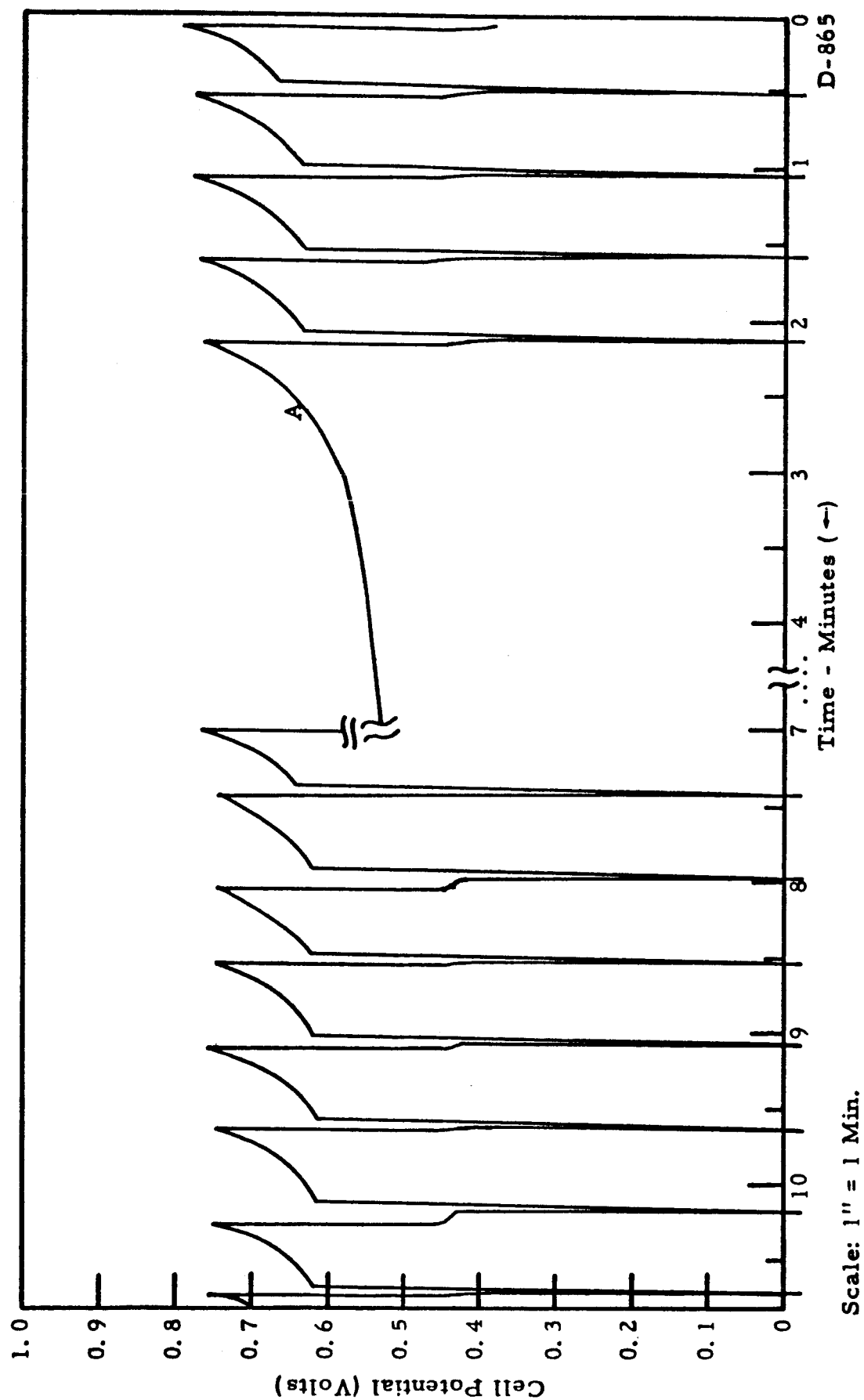


Fig. 28 Comparison Heavy Discharge Pulse and Normal Discharge.

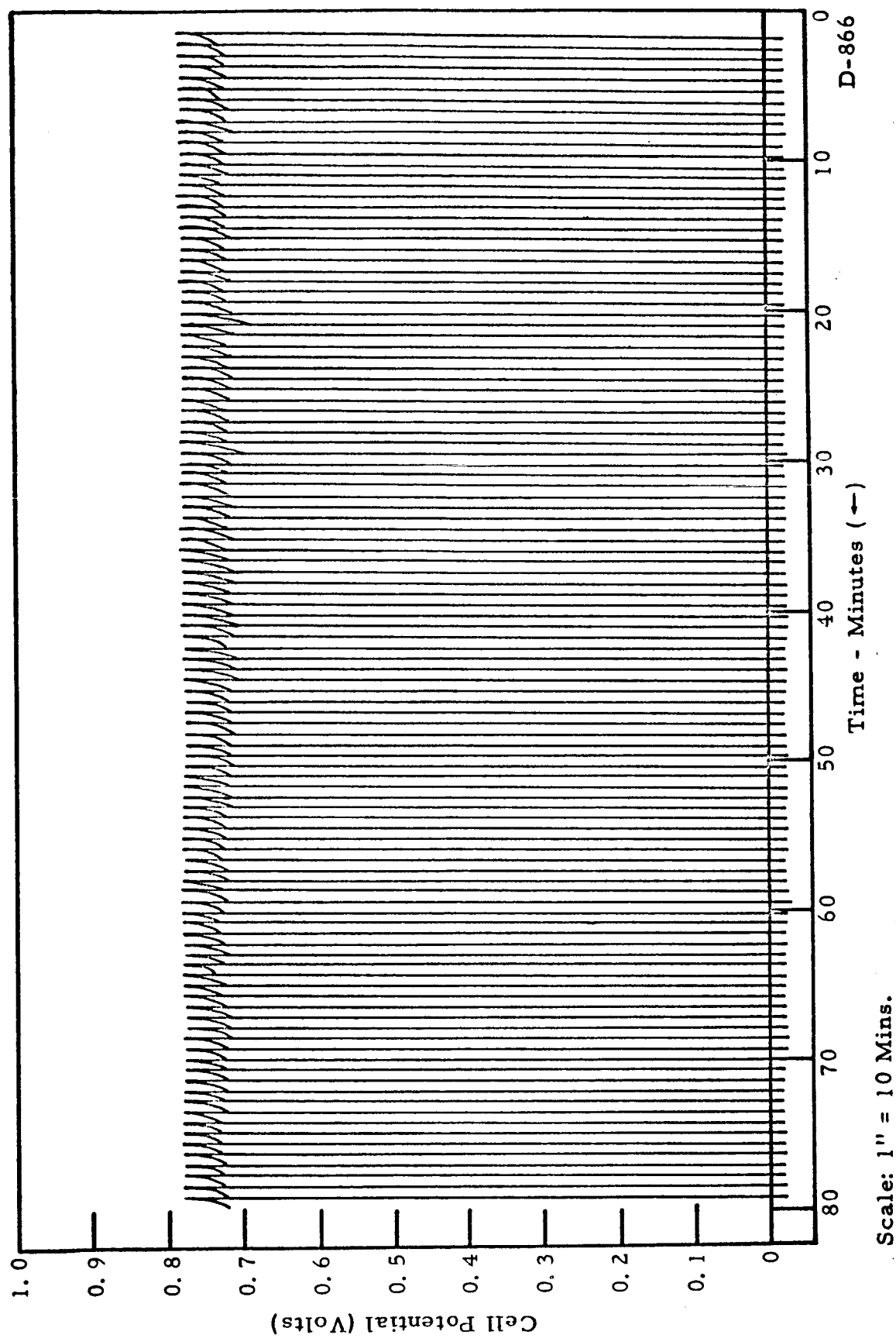


Fig. 29 Cell Voltage Maintained by Heavy Discharge Pulse.